Abstracta

Ano XVII - N. 03

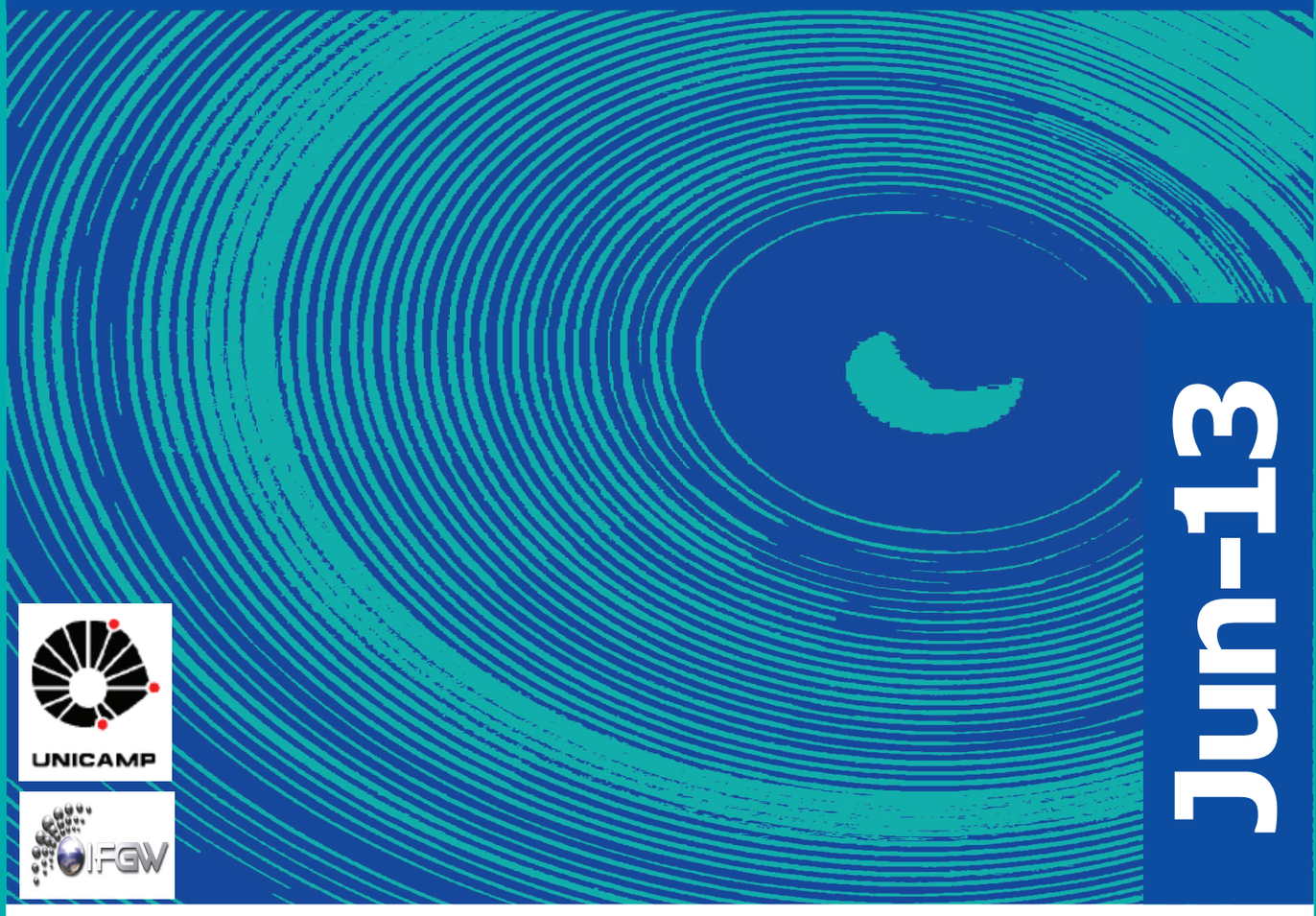

Jun-13

Trabalhos Publicados

[P107-13] "1-Methyl-2-Pyrrolidone: From Exfoliating Solvent to a Paramagnetic Ligand"

Lemus-Santana, A. A.; Gonzalez, M.; Rodriguez-Hernandez, J.; **Knobel, M.***; Reguera, E.

When 1-methyl-2-pyrrolidone molecule (1m2p) interacts with the T[Ni(CN)(4)] layer, its carbonyl g bond homolytically disrupts and forms a coordination bond at the axial positions for the metal T, and hybrid inorganic-organic solids of formula unit T(L)(2)[Ni(CN)(4)], with T = Mn, Co, Ni, are obtained. The formed solids crystallize with a monoclinic unit cell in the C2/m space group where the metal T is found with octahedral coordination to four N ends of CN groups from a given layer and to two oxygen atoms from the organic ligands, while the inner metal (Ni) preserves its square planar coordination. In the interlayer region, the organic molecules achieve unusual planarity and are stacked through dipole-dipole interactions in a head-to-tail configuration to form a chain of molecular pillars. From such interactions, 3D pillared hybrid solids result. Upon the charge donation to the metal by oxygen atom from 1m2p, the latter becomes an organic radical whose SOMO frontier orbital has a strong pi character, associated with an essentially planar structure. The unpaired electron is delocalized between neighboring C and N atoms at the ligand ring plane, and it is featured by an outstanding broad absorption band in the near-IR region. For Ni, the metal of highest polarizing power within the considered series, the existence of pi overlapping interaction between organic ligand molecules leads to ferromagnetic ordering at low temperature, with T-C = 10.07 K. For Mn and Co, related to the lower metal electron-withdrawing ability, the materials maintain the weak antiferromagnetic character resulting from the interaction between T metals in the layer -T-NC Ni-C N-T-chains.

Journal Of Physical Chemistry A 117[11], 2400-2407, 2013. DOI: 10.1021/jp4007813

[P108-13] "A Bright Impulsive Solar Burst Detected At 30 Thz"

Kaufmann, P.; White, S. M.; Freeland, S. L.; **Marcon, R.***; Fernandes, L. O. T.; Kudaka, A. S.; de Souza, R. V.; Aballay, J. L.; Fernandez, G.; Godoy, R.; Marun, A.; Valio, A.; Raulin, J. P.; de Castro, C. G. G.

Ground- and space-based observations of solar flares from radio wavelengths to gamma-rays have produced considerable insights but raised several unsolved controversies. The last unexplored wavelength frontier for solar flares is in the range of submillimeter and infrared wavelengths. Here we report the detection of an intense impulsive burst at 30 THz using a new imaging system. The 30 THz emission exhibited remarkable time coincidence with peaks observed at microwave, mm/submm, visible, EUV, and hard X-ray wavelengths. The emission location coincides with a very weak white-light feature, and is consistent with heating below the temperature minimum in the atmosphere. However, there are problems in attributing the heating to accelerated electrons. The peak 30 THz flux is several times larger than the usual microwave peak near 9 GHz, attributed to non-thermal electrons in the corona. The 30 THz emission could be consistent with an optically thick spectrum increasing from low to high frequencies. It might be part of the same spectral component found at sub-THz frequencies whose nature remains mysterious. Further observations at these wavelengths will provide a new window for flare studies.

Astrophysical Journal 768[2], 134, 2013. DOI: 10.1088/0004-637X/768/2/134

[P109-13] "A simple derivation of the Lindblad equation"

Brasil, C.A.*, Fanchini, F.F., Napolitano, R.J.

We present a derivation of the Lindblad equation - an important tool for the treatment of nonunitary evo- lutions - that is accessible to undergraduate students in physics or mathematics with a basic background on quantum mechanics. We consider a specific case, corresponding to a very simple situation, where a primary system interacts with a bath of harmonic oscillators at zero temperature, with an interaction Hamiltonian that resembles the Jaynes-Cummings format. We start with the Born-Markov equation and, tracing out the bath degrees of freedom, we obtain an equation in the Lindblad form. The specific situation is very instructive, for it makes it easy to realize that the Lindblads represent the effect on the main system caused by the interaction with the bath, and that the Markov approximation is a fundamental condition for the emergence of the Lindbladian operator. The formal derivation of the Lindblad equation for a more general case requires the use of quantum dynamical semi-groups and broader considerations regarding the environment and temperature than we have considered in the particular case treated here.

Revista Brasileira de Ensino de Fisica 35[1], 1303, 2013.

[P110-13] "A single-frequency, diode-pumped Nd:YLF laser at 657 nm: a frequency and intensity noise comparison with an extended cavity diode laser"

Portela, M. N.*; Wetter, N. U.; Zondy, J. J.; **Cruz, F. C.***

We report on a continuous wave, diode-pumped, intracavity frequency-doubled Nd:YLF (yttrium lithium fluoride) single--frequency ring laser designed for high-resolution spectroscopy of the calcium intercombination transition at 657 nm. We measured its frequency modulation (FM) and amplitude modulation (AM) noise and compared it with an extended cavity diode laser (ECDL). The Nd: YLF laser has much lower FM noise, extending to 50 kHz in comparison with 5 MHz for the ECDL, and slightly higher AM noise, transferred from the pump diode laser. This characterization is important for the design of servo-systems for frequency or intensity stabilization, and also for quantum optics experiments. A Nd: YLF laser at 657 nm can become an attractive high-power 'local oscillator' for a calcium optical clock, with a fundamental 'telecom wavelength' that can be directly used for remote transfer in optical fibers.

Laser Physics 23[2], 025801, 2013. DOI: 10.1088/1054-660X/23/2/025801

[P111-13] "Alpha spectrometry study on LR 115 and Makrofol through measurements of track diameter"

Soares, C.J.*, Alencar, I.*, Guedes, S.*, Takizawa, R.H.*, Smilgys, B.*, Hadler, J.C.*

Measurements of alpha track etch-pit diameters (from a 241Am source) are reported for CR-39, LR 115 and Makrofol detectors. The first detector was used to calibrate the source, whereas the possibility of alpha spectroscopy was investigated in the others. A 226Ra source was also used for CR-39 to detect a higher energy (≈6.96 MeV). The data found for CR-39 are in agreement with previous results. LR 115 and Makrofol presented the characteristic Bragg peak, which indicates that these detectors can be used as alpha spectrometers. Finally, within the applied etching conditions, it was possible to observe energy detection windows for LR 115 and Makrofol. For the etching conditions employed in this work, maximum energy thresholds were found to be approximately 4.5 MeV and 3.7 MeV, for LR 115 and Makrofol, respectively. Therefore, our results indicate alpha particle tracks from plated-out radon progeny would be naturally excluded if these detectors were used to monitor environmental radon and its progeny, confirming previous results performed with different experimental conditions.

Radiation Measurements 50, 246-248. DOI: 10.1016/j.radmeas.2012.06.010

[P112-13] "Antimicrobial Cyanopeptide Action on Bacterial Cells Observed with Atomic Force Microscopy"

Silva-Stenico, M. E.; Lorenzi, A. S.; **Teschke, O.***; Silva, C. S. P.; Etchegaray, A.; Fiore, M. F.

Cyanobacteria produce oligopeptides that are predominantly synthesized by the non-ribosomal pathway. Among these are the aeruginosin and cyanopeptolin protease inhibitors, which act against enzymes known to cause several human health problems. Atomic force microscopy (AFM) was used to study the effect of cyanopeptides produced by Microcystis aeruginosa NPCD-1 on pathogenic bacterial cell surfaces. The selected strain was characterized based on the 16S rRNA gene sequence and the intergenic spacer region of the phycocyanin operon. PCR amplification was employed to investigate the presence of genes encoding for aeruginosin and cyanopeptolin. Purified extract from M. aeruginosa NPCD-1 cells was screened for bioactive compounds. The effect of purified extract containing protease inhibitors produced by the NPCD-1 strain on bacterial cells was observed using AFM. Aeruginosin and cyanopeptolin genes were confirmed by both PCR amplification and gene sequencing. Mass spectrometry analysis confirmed the production of aeruginosin. The interaction of Bacillus cereus, Escherichia coli and Staphylococcus aureus with cyanopeptides was characterized by examining the loss of surface stiffness and the formation of micelles, most likely originating from the membrane disruption. The AFM results demonstrate the ability of cyanobacterial extract to alter the cellular membrane of bacterial pathogens.

Current Nanoscience 9[1], 141-148, 2013.

[P113-13] "Assessment of the thermal expansion mismatch in lanthanum strontium cobalt ferrite-yttria stabilized zirconia two-layers systems using photoacoustic methodology"

Guimaraes, A. O.; **Mansanares, A. M.***; Guimaraes, V. F.; Paes, H. R.; Vargas, H.

In this letter we investigate the thermo-elastic mismatch in lanthanum strontium cobalt ferrite (La0.6Sr0.4Co0.2Fe0.8O3--delta) (LSCF) films deposited onto yttria stabilized zirconia (YSZ) substrates, applicable to solid oxide fuel cells. We investigated composite LSCF+YSZ and pure LSCF films deposited onto commercial YSZ substrate. Photoacoustics was used to obtain the effective thermal diffusivity and thermal expansion coefficient of the two-layers samples. Based on a thermal-electrical analogy model, it was possible to get the thermo-elastic properties of the films and to confirm the desired reduction on the thermo-elastic mismatch between film and substrate when comparing composite LSCF+YSZ and pure LSCF films.

Applied Physics Letters 102[13], 131910, 2013. DOI: 10.1063/1.4800064

[P114-13] "Boron thin films and CR-39 detectors in BNCT: A method to measure the 10B(n,α)7Li reaction rate"

Smilgys, B.*, Guedes, S.*, Morales, M.*, Alvarez, F.*, Hadler, J.C.*, Coelho, P.R.P., **Siqueira, P.T.D.*, Alencar, I.*, Soares, C.J.***, Curvo, E.A.C.

The working principle of the Boron Neutron Capture Therapy (BNCT) is the selective delivery of a greater amount of boron to the tumor cells than to the healthy ones, followed by the neutron irradiation that will induce the emission of α-particles and recoil 7Li nuclei through the 10B(n,α)7Li reaction. The objective of this work is to present a setup composed of a boron thin film coupled with CR-39. Alpha and 7Li particle coming from the boron films are used to quantify neutron boron reaction and are detected by CR-39. The nuclei compounding of this detector, H, C and O, will undergo fast neutrons reactions, which will be detected in the CR-39 itself. In this way, the 10B(n,α) 7Li reaction and the contribution of fast neutrons to the flux can be determined at the same time. These measurements are essential for treatment planning as well as for studies of the biodistribution of 10B-carrier drugs and tissue microdosimetry. The boron films were deposited on stainless steel substrates through the sputtering technique and irradiated with thermal neutrons at the reactor IEA-R1 located at IPEN, São Paulo/SP, Brazil. Here we show the first results on the characterization of these thin films and calibration of the proposed setup.

Radiation Measurements 50 181-186, 2013. DOI: 10.1016/j.radmeas.2012.07.001

[P115-13] "Bounds on the density of sources of ultra-high energy cosmic rays from the Pierre Auger Observatory"

Abreu, P., Aglietta, M., Ahlers, M., Ahn, E.J., Albuquerque, I.F.M., **Alves Batista, R.*, Chinellato, J.A.*, Daniel, B.*, De Mello Junior, W.J.M.*, Dobrigkeit, C.*, Escobar, C.O.*, Fauth, A.C.*, Kemp, E.*, Muller, M.A.*, Pakk Selmi-Dei, D.*, Zimbres Silva, M.***

We derive lower bounds on the density of sources of ultra--high energy cosmic rays from the lack of significant clustering in the arrival directions of the highest energy events detected at the Pierre Auger Observatory. The density of uniformly distributed sources of equal intrinsic intensity was found to be larger than (0.06-5) × 10-4 Mpc-3 at 95% CL, depending on the magnitude of the magnetic deflections. Similar bounds, in the range (0.2-7) × 10-4 Mpc-3, were obtained for sources following the local matter distribution.

Journal of Cosmology and Astroparticle Physics 2013[5], 009, 2013. DOI: 10.1088/1475-7516/2013/05/009

[P116-13] "Can we explain why leptonic electroweak interactions are chiral?"

Dartora, C. A.; **Cabrera, G. G.***

One of the fundamental ingredients in the standard model of electroweak interactions between fundamental particles is chirality. Currently there are no hints about why nature has chosen the chiral way. The answer to such a fundamental question could be the extension of the whole theory to the superluminal sector of the Lorentz-Poincare group. Restricting ourselves to leptons, we postulate that the neutrinos are a priori described by a tachyonic Dirac Lagrangian. It could provide a simple explanation for the parity violation in weak interactions and why electroweak theory has a chiral aspect, leading to invariance under a SUL(2) x U-Y(1) gauge group. Right-handed neutrino becomes sterile and decoupled from the other particles quite naturally.

EPL 101[5], 51002, 2013. DOI: 10.1209/0295-5075/101/51002

[P117-13] "Centrality dependence of charged particle production at large transverse momentum in Pb-Pb collisions at root s(NN)=2.76 TeV"

Abelev, B.; Adam, J.; Adamova, D.; Adare, A. M.; Aggarwal, M. M.; **Chinellato, D. D.*; Dash, A.*; Takahashi, J.***; et al.
ALICE Collaboration

The inclusive transverse momentum (p(T)) distributions of primary charged particles are measured in the pseudo-rapidity range vertical bar eta vertical bar <0.8 as a function of event centrality in Pb-Pb collisions at root S-NN = 2.76 TeV with ALICE at the LHC.

The data are presented in the p(T) range 0.15 < p(T) <50 GeV/c for nine centrality intervals from 70-80% to 0-5%. The results in Pb-Pb are presented in terms of the nuclear modification factor R-AA using a pp reference spectrum measured at the same collision energy. We observe that the suppression of high--p(T) particles strongly depends on event centrality. The yield is most suppressed in central collisions (0-5%) with R-AA approximate to 0.13 at p(T) = 6-7 GeV/c. Above p(T) = 7 GeV/c, there is a significant rise in the nuclear modification factor, which reaches R-AA approximate to 0.4 for p(T) > 30 GeV/c. In peripheral collisions (70-80%), only moderate suppression (R-AA approximate to 0.6-0.7) and a weak p(T) dependence is observed. The measured nuclear modification factors are compared to other measurements and model calculations.

Physics Letters B 720[1-3], 52-62, 2013. DOI: 10.1016/j.physletb.2013.01.051

[P118-13] "Charged kaon femtoscopic correlations in pp collisions at root s=7 TeV"

Abelev, B.; Adam, J.; Adamova, D.; Adare, A. M.; Aggarwal, M. M.; **Dash, A.*; Takahashi, J.***; et al.
ALICE Collaboration

Correlations of two charged identical kaons (KchKch) are measured in pp collisions at root s = 7 TeV by the ALICE experiment at the Large Hadron Collider (LHC). One-dimensional (KKch)-K-ch correlation functions are constructed in three multiplicity and four transverse momentum ranges. The (KKch)-K-ch femtoscopic source parameters R and lambda are extracted. The (KKch)-K-ch correlations show a slight increase of femtoscopic radii with increasing multiplicity and a slight decrease of radii with increasing transverse momentum. These trends are similar to the ones observed for pi pi and K-s(0) K-s(0) correlations in pp and heavy-ion collisions. However at high multiplicities, there is an indication that the one-dimensional correlation radii for charged kaons are larger than those for pions in contrast to what was observed in heavy-ion collisions at the Relativistic Heavy-Ion Collider.

Physical Review D 87[5], 052016, 2013. DOI: 10.1103/PhysRevD.87.052016

[P119-13] "Coercivity behavior in Gd(Co1-xCux)(5) system as function of the microstructure evolution"

Penton-Madrigal, A.; **de Oliveira, L. A. S.***; Sinnecker, J. P.; Souza, D. M.; Grossinger, R.; Concepcion-Rosabal, B.; Estevez--Rams, E.; Diaz-Castanon, S.

Magnetic measurements, X-ray diffraction and scanning electron microscopy (SEM) experiments were carried out in the as--cast Gd(Co1-xCux)(5) samples with different Co/Cu content. Already in the as cast state, this system shows high coercive field for x = 0.3 and a magnetization driven by nucleation of reversal domain. SEM micrograph and microanalysis show possible spinodal decomposition in the as-cast state, hence regions with different Co/Cu-content are observed, while the Gd-content almost does not change. High resolution X-ray diffraction patterns show a main CaCu5-type structure with traces of a secondary phase and distorted peak profiles as function of the Cu content. The evolution of the microstructure is discussed in relation with the Cu incorporation into the CaCu5-type structure. The Cu addition avoids the formation of the 2:7 phase within the 1:5 matrix, favoring the formation of a more homogeneous Gd(Co, Cu)(5) phase. The relation between the observed microstructure and the magnetic behavior is also discussed.

Physica B-Condensed Matter 414, 67-71, 2013. DOI: 10.1016/j.physb.2013.01.024

[P120-13] "Coherent J/psi photoproduction in ultra-peripheral Pb-Pb collisions at root s(NN)=2.76 TeV"

Abelev, B.; Adam, J.; Adamova, D.; Adare, A. M.; Aggarwal, M. M.; **Dash, A.*; Takahashi, J.***; et al.
ALICE Collaboration

The ALICE Collaboration has made the first measurement at the LHC of J/psi photoproduction in ultra-peripheral Pb--Pb collisions at root s(NN) = 2.76 TeV. The J/psi is identified via its dimuon decay in the forward rapidity region with the muon spectrometer for events where the hadronic activity is required to be minimal. The analysis is based on an event sample corresponding to an integrated luminosity of about 55 mu b(-1). The cross section for coherent J/psi production in the rapidity interval -3.6 < y < -2.6 is measured to be d sigma(coh)(J/psi)/dy = 1.00 +/- 0.18(stat)(-0.26)(+0.24)(syst) mb. The result is compared to theoretical models for coherent J/psi production and found to be in good agreement with those models which include nuclear gluon shadowing.

Physics Letters B 718[4-5], 1273-1283, 2013. DOI: 10.1016/j.physletb.2012.11.059

[P121-13] "Compensation effect on the CW spin-polarization degree of Mn-based structures"

Balanta, M.A.G.*, Brasil, M.J.S.P.*, Iikawa, F.*, Mendes, U.C.*, Brum, J.A.*, Maialle, M.Z., Danilov, Yu.A., Vikhrova, O.V., Zvonkov, B.N.

We investigated the effects of Mn ions on the spin dynamics of electrons confined in a semiconductor quantum well nearby a Mn-based ferromagnetic layer. Circularly polarized Hanle and time-resolved photoluminescence (PL) measurements were carried out on a set of samples with different Mn delta-doping concentrations. We observe a strong influence of the Mn layer for both the electron lifetime and its spin-relaxation time for high-Mn concentrations, when the electrons significantly overlap with Mn ions. Our results also show that the circular-polarization degree obtained by simple continuous-wave PL measurements is not sufficient to determine the relaxation dynamics due to a compensation effect of the lifetime and the spin-relaxation time.

Journal of Physics D: Applied Physics 46[21], 215103, 2013. DOI: 10.1088/0022-3727/46/21/215103

[P122-13] "Conduction electron spin resonance in AlB2"

Holanda, L.M.*, Mendonça-Ferreira, L., Ribeiro, R.A., Osorio--Guillén, J.M., Dalpian, G.M., Kuga, K., Nakatsuji, S., Fisk, Z., **Urbano, R.R.*, Pagliuso, P.G.*, Rettori, C.***

This work reports on electron spin resonance experiments in oriented single crystals of the hexagonal AlB2 diboride compound (P6/mmm, D16h structure) which display conduction electron spin resonance. The X-band electron spin resonance spectra showed a metallic Dysonian resonance with g-value and intensity independent of temperature. The thermal broadening of the anisotropic electron spin resonance linewidth ΔH tracks the T-dependence of the electrical resistivity below T ~ 100 K. These results confirm the observation of a conduction electron spin resonance in AlB2 and are discussed in comparison with other boride compounds. Based on our main findings for AlB2 and the calculated electronic structure of similar layered honeycomb-like structures, we conclude that any array of covalent B-B layers potentially results in a conduction electron spin resonance signal. This observation may shed new light on the nature of the non-trivial conduction electron spin resonance-like signals of complex f-electron systems such as ß-YbAlB4.

Journal of Physics Condensed Matter 25[21], 216001, 2013. DOI: 10.1088/0953-8984/25/21/216001

[P123-13] "Cross sections for electron scattering by formaldehyde and pyrimidine in the low- and intermediate--energy ranges"

Ferraz, J. R.; dos Santos, A. S.; de Souza, G. L. C.; Zanelato, A. I.; Alves, T. R. M.; Lee, M. T.; **Brescansin, L. M.***; Lucchese, R. R.; Machado, L. E.

We report a theoretical study on electron scattering by two strongly polar molecules, namely, formaldehyde (CH2O) and pyrimidine (C4H4N2), in the low-and intermediate-energy ranges. Calculated elastic differential, integral, and momentum--transfer cross sections, as well as total (elastic + inelastic) and total absorption cross sections, are reported for impact energies ranging from 0.2 to 500 eV. A complex optical potential is used to represent the electron-molecule interaction dynamics, whereas a single-center-expansion method associated with the Pade approximant technique is used to solve the scattering equations. Our calculated results are compared with experimental results and other theoretical data available in the literature. Generally good agreement is seen in these comparisons.

Physical Review A 87[3], 032717, 2013. DOI: 10.1103/PhysRevA.87.032717

[P124-13] "Cross sections for positron scattering from ethane"

Chiari, L.; Zecca, A.; Trainotti, E.; Bettega, M. H. F.; Sanchez, S. D.; Varella, M. T. N.; **Lima, M. A. P.***; Brunger, M. J.

We report experimental and theoretical cross sections for positron scattering from the fundamental organic-chemistry molecule ethane (C2H6). The experimental total cross sections (TCSs) were obtained using a linear transmission technique, for energies in the range 0.1-70 eV and with an energy resolution of similar to 0.25 eV (full width at half maximum). Agreement, over the common energy range, with the earlier TCS measurements of Floeder et al. [J. Phys. B 18, 3347 (1985)] is excellent, while both the present results and those of Floeder et al. are consistently higher in magnitude than the data of Sueoka and Mori [J. Phys. B 19, 4035 (1986)]. The present calculations employed the Schwinger multichannel method and were performed in the static plus polarization approximation for energies up to 10 eV. Our calculated elastic integral cross sections (ICSs) indicate a Ramsauer-Townsend minimum at around 1.4 eV in the A(g) scattering symmetry, and a virtual state. In addition we calculated from our scattering cross section a scattering length of -13.83a(0). Agreement between our measured TCS and calculated elastic ICS is found to be only qualitative, although this is perhaps not so surprising given the TCS below 10 eV in principle includes contributions from rotational, vibrational, and electronic-state excitation and positronium formation whereas the calculation does not.

Physical Review A 87[3], 032707, 2013. DOI: 10.1103/PhysRevA.87.032707

[P125-13] "Decomposition of Lignin from Sugar Cane Bagasse during Ozonation Process Monitored by Optical and Mass Spectrometries"

Souza-Correa, J. A.; **Ridenti, M. A.***; Oliveira, C.; Araujo, S. R.; **Amorim, J.***

Mass spectrometry was used to monitor neutral chemical species from sugar cane bagasse that could volatilize during the bagasse ozonation process. Lignin fragments and some radicals liberated by direct ozone reaction with the biomass structure were detected. Ozone density was monitored during the ozonation by optical absorption spectroscopy. The optical results indicated that the ozone interaction with the bagasse material was better for bagasse particle sizes less than or equal to 0.5 mm. Both techniques have shown that the best condition for the ozone diffusion in the bagasse was at 50% of its moisture content. In addition, Fourier transform infrared spectroscopy (FTIR) and scanning electron microscopy (SEM) were employed to analyze the lignin bond disruptions and morphology changes of the bagasse surface that occurred due to the ozonolysis reactions as well. Appropriate chemical characterization of the lignin content in bagasse before and after its ozonation was also carried out.

Journal Of Physical Chemistry B 117[11], 3110-3119, 2013. DOI: 10.1021/jp3121879

[P126-13] "Dependence of the magnetocaloric effect on the A-site ionic radius in isoelectronic manganites"

Rocco, D. L.; **Coelho, A. A.***; Gama, S.; Santos, M. D.

In this work, we explore the magnetocaloric and magnetic properties of isoelectronic manganites R0.6Sr0.4MnO3 (R = La, Pr, Nd, and Sm). Upon substitution of La3+ by smaller rare-earth ions, the average ionic radius < r(A)> of the A-site (A = (R, Sr)) elements systematically decreases. It is found that, with decreasing < r(A)>, the magnetic-ordering temperature decreases from 341K for La0.6Sr0.4MnO3 to 126K for Sm0.6Sr0.4MnO3. Interestingly, the magnetic-entropy change increases with decreasing < r(A)>, reaching Delta S-M = - 8: 4 J/kg K for Delta H = 0 - 20 kOe for Sm0.6Sr0.4MnO3. For manganites, this is a high value of DSM, and it is related to the fact that the compound exhibits first-order magnetic transition. In contrast, the three other compounds exhibit a second order transition. The results indicate that the structural distortions caused by the decreasing < r(A)> couple the spin subsystem to the lattice, thus, inducing a first-order magnetic transition.

Journal Of Applied Physics 113[11], 113907, 2013. DOI: 10.1063/1.4795769

[P127-13] "Dielectric resonator antenna for applications in nanophotonics"

Malheiros-Silveira, G. N.; **Wiederhecker, G. S.***; Hernandez--Figueroa, H. E.

Optical nanoantennas, especially of the dipole type, have been theoretically and experimentally demonstrated by many research groups. Likewise, the plasmonic waveguides and optical circuits have experienced significant advances. In radio frequencies and microwaves a category of antenna known as dielectric resonator antenna (DRA), whose radiant element is a dielectric resonator (DR), has been designed for several applications, including satellite and radar systems. In this letter, we explore the possibilities and advantages to design nano DRAs (NDRAs), i.e., DRAs for nanophotonics applications. Numerical demonstrations showing the fundamental antenna parameters for a circular cylindrical NDRA type have been carried out for the short (S), conventional (C), and long (L) bands of the optical communication spectrum.

Optics Express 21[1], 1234-1239, 2013

[P128-13] "Drifting electron excitation of acoustic phonons: Cerenkov-like effect in n-GaN"

Rodrigues, C. G.; **Vasconcellos, A. R.*; Luzzi, R.***

The process of generation of acoustic phonons by way of drifting electron excitation in polar semiconductors is considered. Similarly to what is present in LO phonons, the emergence of a condensation of the pumped energy in modes around an off-center region of the Brillouin zone is evidenced. The phonons are emitted within a lobe-like distribution with an axis along the direction of the electric field.

A numerical calculation for the case of GaN is done, which shows that the phenomenon can be largely enhanced at high carrier densities and in strong piezoelectric materials.

Journal Of Applied Physics 113[11], 113701, 2013. DOI: 10.1063/1.4795271

[P129-13] "Effects of a He-3 impurity on the Elastic Anomalies of He-4 at T=0"

Pessoa, R.; **Vitiello, S. A.***

Effects on the elastic constants of a system formed from He-4 atoms with a He-3 impurity concentration of 0.14 % are investigated in a range of densities varying from 0.029 to 0.035 (-3). A model wave function of the shadow class is used to compute elastic constants and quantities defined through relations satisfied by them. The linear compressibility assumes the isotropic character expected for an hcp crystal with a constant value of the structure axis ratio c/a. This is in contrast with bulk He-4 where an anisotropic behavior is observed.

Journal Of Low Temperature Physics 171[3-4], 315-321, 2013. DOI: 10.1007/s10909-012-0739-8

[P130-13] "Effects of initial state fluctuations in the final state elliptic flow measurements using the NeXSPheRIO model"

de Souza, R. D.*; Takahashi, J.*; Kodama, T.; Sorensen, P.

We present a systematic study of the effects from initial condition fluctuations in systems formed by heavy-ion collisions using the hydrodynamical simulation code NeXSPheRIO. The study was based on a sample of events generated simulating Au + Au collisions at center-of-mass energy of 200 GeV per nucleon pair with an impact parameter ranging from most central to peripheral collisions. The capability of the NeXSPheRIO code to control and save the initial condition (IC) as well as the final state particles after the three-dimensional hydrodynamical evolution allows for the investigation of the sensitivity of the experimental observables to the characteristics of the early IC. Comparisons of results from simulated events generated using fluctuating initial conditions and a smooth initial condition are presented for the experimental observable elliptic flow parameter (v(2)) as a function of the transverse momentum p(t) and centrality. We compare v(2) values estimated using different methods, and how each method responds to the effects of fluctuations in the initial condition. Finally, we quantify the flow fluctuations and compare them to the fluctuations of the initial eccentricity of the energy density distribution in the transverse plane.

Physical Review C 85[5], 054909, 2012. DOI: 10.1103/PhysRevC.85.054909

[P131-13] "Electron collisions with the HCOOH(H2O)n complexes (n = 1, 2) in liquid phase: The influence of microsolvation on the π resonance of formic acid"

Freitas, T.C., **Coutinho, K.*, Varella, M.T.D.N.***, **Lima, M.A.P.***, **Canuto, S.***, Bettega, M.H.F.

We report momentum transfer cross sections for elastic collisions of low-energy electrons with the HCOOH(H2O)n complexes, with n 1, 2, in liquid phase. The scattering cross sections were computed using the Schwinger multichannel method with pseudopotentials in the static-exchange and static-exchange plus polarization approximations, for energies ranging from 0.5 eV to 6 eV. We considered ten different structures of HCOOH-H2O and six structures of HCOOH(H2O)2 which were generated using classical Monte Carlo simulations of formic acid in aqueous solution at normal conditions of temperature and pressure. The aim of this work is to investigate the influence of microsolvation on the π shape resonance of formic acid. Previous theoretical and experimental studies reported a π shape resonance for HCOOH at around 1.9 eV. This resonance can be either more stable or less stable in comparison to the isolated molecule depending on the complex structure and the water role played in the hydrogen bond interaction. This behavior is explained in terms of (i) the polarization of the formic acid molecule due to the water molecules and (ii) the net charge of the solute. The proton donor or acceptor character of the water molecules in the hydrogen bond is important for understanding the stabilization versus destabilization of the π resonances in the complexes. Our results indicate that the surrounding water molecules may affect the lifetime of the π resonance and hence the processes driven by this anion state, such as the dissociative electron attachment.

Journal of Chemical Physics 138[17], 174307, 2013. DOI: 10.1063/1.4803119

[P132-13] "Electron Neutrino and Antineutrino Appearance in the Full MINOS Data Sample"

Adamson, P.; Anghel, I.; Backhouse, C.; Barr, G.; Bishai, M.; Blake, A.; **Coelho, J. A. B.*; Escobar, C. O.***; et al.
MINOS Collaboration

We report on v(e) and (v) over bar (e) appearance in v(mu) and (v) over bar (mu) beams using the full MINOS data sample. The comparison of these v(e) and (v) over bar (e) appearance data at a 735 km baseline with theta(13) measurements by reactor experiments probes delta, the theta(23) octant degeneracy, and the mass hierarchy. This analysis is the first use of this technique and includes the first accelerator long--baseline search for (v) over bar (mu) -> (v) over bar (e). Our data disfavor 31% (5%) of the three-parameter space defined by delta, the octant of the theta(23), and the mass hierarchy at the 68% (90%) C.L. We measure a value of 2sin(2)(2 theta(13)) sin(2)(theta(23)) that is consistent with reactor experiments.

Physical Review Letters 110[17], 171801, 2013. DOI: 10.1103/PhysRevLett.110.171801

[P133-13] "Electronic localization at mesoscopic length scales: different definitions of localization and contact effects in a heuristic DNA model"

Paez, C. J.*; Schulz, P. A.*

In this work we investigate the electronic transport along model disordered DNA molecules using an effective tight-binding approach, addressing the localization properties. Different tools to investigate the degree of localization are examined as a function of system length, energy dependence and DNA to electrode coupling: localization length, participation number and sensitivity to boundary conditions. Combining the results obtained from these different tools, a thermodynamic limit for the model DNA molecule, within the mesoscopic length scale, can be established. Furthermore, three aspects are investigated: (i) the influence of strongly localized resonances on the localization length is discussed as an important mechanism defining the degree of localization for sizes below the thermodynamic limit; (ii) the dependence on the Hamiltonian parameters on a possible diffusive regime for short systems; and, finally, (iii) possible length dependent origins for the large discrepancies among experimental results for the electronic transport in DNA samples.

European Physical Journal B 86[3], 103, 2013. DOI: 10.1140/epjb/e2013-30728-9

[P134-13] "Erbium enhanced formation and growth of photoluminescent Er/Si nanocrystals"

Mustafa, D., Biggemann, D., Martens, J.A., Kirschhock, C.E.A., **Tessler, L.R.***, Breynaert, E.

Photoluminescent Er/Si-nanocrystal composites were obtained after annealing Er doped silicon suboxide (SiOx) thin films. The films were prepared by reactive sputtering (Ar/O2 atmosphere) with a pure silicon target partially covered with metallic Er. The presence of Er in the resulting films strongly influences Si nanocrystal nucleation and growth during thermal treatment at temperatures between 300 and 1300 C. A correlation between Er photoluminescence (PL) spectra, Er speciation and Si nanocrystal properties indicated that PL bands and their intensity are directly influenced by the nanocrystal size and density, and their vicinity to the Er3 + centers. This correlation is explained by considering Er centers as promotor for SiOx disproportionation, locally increasing Si0 concentration which leads to formation of Si nanocrystals in the vicinity of Er.

Thin Solid Films 536, 196-201, 2013. DOI: 10.1016/j.tsf.2013.03.027

[P135-13] "Evolution and stability of ring species"

Martins, A. B.; **de Aguiar, M. A. M.***; Bar-Yam, Y.

Neutral models, in which genetic change arises through random variation without fitness differences, have proven remarkably successful in describing observed patterns of biodiversity, despite the manifest role of selection in evolution. Here we investigate the effect of barriers on biodiversity by simulating the expansion of a population around a barrier to form a ring species, in which the two ends of the population are reproductively isolated despite ongoing gene flow around the ring. We compare the spatial and genetic properties of a neutral agent-based population model to the greenish warblers' complex, a well-documented example of an actual ring species in nature. Our results match the distribution of subspecies, the principal components of genetic diversity, and the linear spatial-genetic correlation of the observed data, even though selection is expected to be important for traits of this species. We find that ring species are often unstable to speciation or mixing but can persist for extended times depending on species and landscape features. For the greenish warblers, our analysis implies that the expanded area near the point of secondary contact is important for extending the duration of the ring, and thus, for the opportunity to observe this ring species. Nevertheless it also suggests the ring will break up into multiple species in 10,000 to 50,000 y. These results imply that simulations can be used to accurately describe empirical data for complex spatial-genetic traits of an individual species.

Proceedings Of The National Academy Of Sciences Of The United States Of America 110[13], 5080-5084, 2013. DOI: 10.1073/pnas.1217034110

[P136-13] "Exchange-bias-like effect in Pr0.75Tb0.25Al 2 and Pr0.7Tb0.3Al2 samples"

Tedesco, J.C.G.*, Pires, M.J.M., Carvalho, A.M.G., De Sousa, V.S.R., **Cardoso, L.P.*, Coelho, A.A.***

The magnetic behavior of pseudobinary Pr0.7Tb 0.3Al2 and Pr0.75Tb0.25Al 2 compounds was studied, and a predominant ferrimagnetic ordering was observed. Noteworthy characteristics such as negative magnetization, compensation points and exchange-bias-like (EB-like) effect were found. This EB-like effect was observed at temperatures below the compensation points. The effect is somewhat different from the one already studied in similar systems combining light and heavy rare earths. The results indicate that the EB-like effect characteristics are related to the conduction electron magnetic polarization and an induced unidirectional anisotropy present in these compounds.

Journal of Magnetism and Magnetic Materials 339, 6-10, 2013. DOI: 10.1016/j.jmmm.2013.02.049

[P137-13] "Experimental studies of di-jets in Au plus Au collisions using angular correlations with respect to back--to-back leading hadrons"

Adamczyk, L.; Agakishiev, G.; Aggarwal, Aggarwal, M. M.; **Derradi de Souza, R.*; Takahashi, J.*; Vasconcelos, G. M. S.***; et al.
STAR Collaboration

Jet-medium interactions are studied via a multihadron correlation technique (called "2 + 1"), where a pair of back-to-back hadron triggers with large transverse momentum is used as a proxy for a di-jet. This work extends the previous analysis for nearly symmetric trigger pairs with the highest momentum threshold of trigger hadron of 5 GeV/c with the new calorimeter-based triggers with energy thresholds of up to 10 GeV and above. The distributions of associated hadrons are studied in terms of correlation shapes and per-trigger yields on each trigger side. In contrast with di-hadron correlation results with single triggers, the associated hadron distributions for back--to-back triggers from central Au + Au data at root S-NN = 200 GeV show no strong modifications compared to d + Au data at the same energy. An imbalance in the total transverse momentum between hadrons attributed to the near-side and away--side of jetlike peaks is observed. The relative imbalance in the Au + Au measurement with respect to d + Au reference is found to increase with the asymmetry of the trigger pair, consistent with the expectation from medium-induced energy-loss effects. In addition, this relative total transverse momentum imbalance is found to decrease for softer associated hadrons. Such evolution indicates that the energy missing at higher associated momenta is converted into softer hadrons.

Physical Review C 87[4], 044903, 2013. DOI: 10.1103/PhysRevC.87.044903

[P138-13] "Extrapolation of zircon fission-track annealing models"

Palissari, R.*, Guedes, S.*, Curvo, E.A.C., **Moreira, P.A.F.P.***, Tello, C.A., **Hadler, J.C.***

One of the purposes of this study is to give further constraints on the temperature range of the zircon partial annealing zone over a geological time scale using data from borehole zircon samples, which have experienced stable temperatures for ~1 Ma. In this way, the extrapolation problem is explicitly addressed by fitting the zircon annealing models with geological timescale data. Several empirical model formulations have been proposed to perform these calibrations and have been compared in this work. The basic form proposed for annealing models is the Arrhenius-type model. There are other annealing models, that are based on the same general formulation. These empirical model equations have been preferred due to the great number of phenomena from track formation to chemical etching that are not well understood. However, there are two other models, which try to establish a direct correlation between their parameters and the related phenomena. To compare the response of the different annealing models, thermal indexes, such as closure temperature, total annealing temperature and the partial annealing zone, have been calculated and compared with field evidence. After comparing the different models, it was concluded that the fanning curvilinear models yield the best agreement between predicted index temperatures and field evidence.

Radiation Measurements 50, 192-196, 2013. DOI: 10.1016/j.radmeas.2012.06.004

[P139-13] "Fe valence fluctuations and magnetoelastic coupling in Pb-based multiferroics perovskites"

Fraygola, B.; Mesquita, A.; **Coelho, A. A.***; Garcia, D.; Mastelaro, V. R.; Eiras, J. A.

Lead-based multiferroics perovskites with nominal compositions Pb(Fe1/2Nb1/2)O-3 and Pb(Fe2/3W1/3)O-3 were synthesized following a two-stage method. Magnetic proprieties were investigated and correlated to anelastic proprieties, measured by the conventional pulse-echo method. The discussions are focused in the region around 250 K, where magnetoelectroe--lastic instabilities have been observed. X-ray absorption near--edge structure (XANES) study further indicates that the edge position varies with temperature revealing a fluctuation on the valence of iron ions with the temperature, which can be related to a variation in anelastic and magnetic proprieties.

Physica Status Solidi A-Applications And Materials Science 210[2], 386-390, 2013. DOI: 10.1002/pssa.201228376

[P140-13] "From quenched to unquenched orbital magnetic moment on metallic@oxide nanoparticles: Dc magnetic properties and electronic correlation"

Muraca, D.*, De Siervo, A.*, Pirota, K.R.*

In this study, the correlation between magnetic, structure, and electronic properties of Ag@Fe3O4 hetero nanostructures are presented. These nanostructures were prepared using a two-step new chemical approach. Three different nanoparticle systems with different Ag concentrations have been prepared and characterized using high resolution transmission electron microscopy, dc magnetization (magnetization and coercive field as a function of temperature), X-ray absorption near edge spectroscopy, and magnetic circular dichroism studies (XMCD). From the correlation between XMCD and dc magnetic measurements (Verwey transition) the presence of non-stoichiometric magnetite in Ag@Fe3O4 nanoparticle systems was confirmed. From the spin and orbital contribution to the total magnetic moment, we conclude that the sample with less Ag seeds particle concentration presents a non-quenched orbital contribution. These phenomena were analyzed based on the actual models and correlated with dc magnetic properties. From these, we conclude that the enhancement on the orbital contribution increases the spin orbital interaction, also increasing the magnetocrystalline anisotropy reflected on the dc magnetic properties.

Journal of Nanoparticle Research 15[1], 1375, 2013. DOI: 10.1007/s11051-012-1375-6

[P141-13] "How Much Time Does a Measurement Take?"

Brasil, C. A.*; de Castro, L. A.; Napolitano, R. D. J.

We consider the problem of measurement using the Lindblad equation, which allows the introduction of time in the interaction between the measured system and the measurement apparatus. We use analytic results, valid for weak system--environment coupling, obtained for a two-level system in contact with a measurer (Markovian interaction) and a thermal bath (non-Markovian interaction), where the measured observable may or may not commute with the system-environment interaction. Analysing the behavior of the coherence, which tends to a value asymptotically close to zero, we obtain an expression for the time of measurement which depends only on the system-measurer coupling, and which does not depend on whether the observable commutes with the system-bath interaction. The behavior of the coherences in the case of strong system-environment coupling, found numerically, indicates that an increase in this coupling decreases the measurement time, thus allowing our expression to be considered the upper limit for the duration of the process.

Foundations Of Physics 43[5], 642-655, 2013. DOI: 10.1007/s10701-013-9707-7

[P142-13] "In-line one-pump parametric amplifier with independent polarization gain: A field-trial demonstration"

Marconi, J. D.*; Fugihara, M. C.*; Callegari, F. A.*; Fragnito, H. L.*

We present a one-pump parametric amplifier with polarization independent gain working as an in-line amplifier within an experimental field-trial optical network. The polarization independent gain is obtained by using a polarization diversity technique (PDT). Five signals modulated at 10 Gb/s were transmitted through the network, and a gain variation as low as 0.05 dB, independent of the signal polarization, was obtained. The bit-error-rate (BER) for the amplified signals was measured. For a BER of 109, a power penalty as low as 0.7 dB is shown. These measurements were compared with the identical ones obtained when the parametric amplifier with the PDT was replaced by an Erbium-doped fiber amplifier (EDFA). The fiber optical parametric amplifier (FOPA) with the PDT presents a power penalty of 0.7 dB in relation to the value obtained with the EDFA. These results show that parametric amplifiers that use the PDT are able to reach a performance comparable to those obtained with the current technology of optical amplifiers based on rare earth doped fibers.

Microwave And Optical Technology Letters 55[5], 1104-1107, 2013. DOI: 10.1002/mop.27481

[P143-13] "Influence of the structure and composition of titanium nitride substrates on carbon nanotubes grown by chemical vapour deposition"

Morales, M.*; Cucatti, S.*; Acuna, J. J. S.; Zagonel, L. F.; Antonin, O.; Hugon, M. C.; Marsot, N.; Bouchet-Fabre, B.; Minea, T.; **Alvarez, F.***

The influence of nano-structure and composition of the substrate on the properties of carbon nanotubes (CNTs) is presented. The samples are obtained following a sequential in situ deposition routine. First, TiNxOy films are grown on a crystalline silicon substrate. Immediately, dispersed nickel catalyst particles are deposited on the film. The non-stoichiometric TiNxOy films and Ni particles are grown by ion beam sputtering of Ti and Ni targets, respectively. Soon after that, the CNTs are grown by feeding acetylene gas into the chamber and maintaining the substrate at 973 K. In situ x-ray photoelectron spectroscopy allows compositional and structural analysis in all the stages of the sample growth process. The CNTs are further studied by scanning and transmission electron microscopy techniques, showing different population densities, sizes and diameters as a function of the oxygen content in the TiNxOy films. The results show that oxygen influences the surface diffusion mobility of the precursor carbon atoms involved in the growth of nanotubes suggesting the inhibition of catalyst particle coarsening. It is concluded that, in addition to acting as a diffusion barrier between the catalyst particles and the silicon support, the TiNxOy films modify the growth kinetics of the CNTs.

Journal Of Physics D-Applied Physics 46[15], 155308, 2013. DOI: 10.1088/0022-3727/46/15/155308

[P144-13] "International collaborations between research universities: experiences and best practices"

Knobel, M.*; Simoes, T. P.*; Cruz, C. H. de*

The world science scenario has observed, in recent years, an important transformation. With the advent of fairly complete publication databases and the improvement of the Internet a number of world university rankings were created, with a clear bias towards research universities. Also, a new field of scientometrics has been developed, and recent studies have clearly demonstrated that the impact of a publication increases if it is written by authors of more than one country.

A general overview of the research collaboration landscape is presented, considering the advantages and problems of international cooperation and the role of research universities. In particular, the case of Ibero-America is explained, with a detailed focus on Brazil. Some interesting practices that have been introduced to improve the degree of internationalization of Brazilian science are shown and discussed.

Studies In Higher Education 38[3], SI, 405-424, 2013. DOI: 10.1080/03075079.2013.773793

[P145-13] "Large magnetocaloric effect and refrigerant capacity near room temperature in as-cast Gd5Ge2Si2-xSnx compounds"

Carvalho, A.M.G., **Tedesco, J.C.G.***, Pires, M.J.M., Soffner, M.E., Guimarães, A.O., **Mansanares, A.M.*, Coelho, A.A.***

Large values of isothermal entropy change (ΔST) and refrigerant capacity have been found in Gd5Ge2Si 2-xSnx compounds. Values of the order of 20 J kg -1 K-1 for -ΔST were obtained in as-cast samples when submitted to a magnetic field variation of 2 T. First-order-magneto-structural transition is induced by the substitution of silicon by tin and it is shifted to lower temperatures with the tin content. It means that the magnetocaloric effect on this series can be properly tuned to a specific practical thermodynamic cycle, including near room temperature range.

Applied Physics Letters 102[19], 192410, 2013. DOI: 10.1063/1.4806971

[P146-13] "Magnetic characteristics of nanocrystalline GaMnN films deposited by reactive sputtering"

Leite, D. M. G.; Pereira, A. L. J.; **Iwamoto, W. A.*; Pagliuso, P. G.***; Lisboa, P. N.; da Silva, J. H. D.

The magnetic characteristics of Ga1-xMnxN nanocrystalline films (x = 0.08 and x = 0.18), grown by reactive sputtering onto amorphous silica substrates (a-SiO2), are shown. Further than the dominant paramagnetic-like behaviour, both field- and temperature-dependent magnetization curves presented some particular features indicating the presence of secondary magnetic phases. A simple and qualitative analysis based on the Brillouin function assisted the interpretation of these secondary magnetic contributions, which were tentatively attributed to antiferromagnetic and ferromagnetic phases.

Solid State Sciences 17, 97-101, 2013. DOI: 10.1016/j.solidstatesciences.2012.11.020

[P147-13] "Measurement of associated production of vector bosons and top quark-antiquark pairs in pp collisions at root s=7 TeV"

Chatrchyan, S.; Khachatryan, V.; Sirunyan, A. M.; Tumasyan, A.; Adam, W.; **Chinellato, J.***; et al.
CMS Collaboration

The first measurement of vector-boson production associated with a top quark-antiquark pair in proton-proton collisions at root s = 7 TeV is presented. The results are based on a data set corresponding to an integrated luminosity of 5.0 fb(-1), recorded by the CMS detector at the LHC in 2011. The measurement is performed in two independent channels through a trilepton analysis of t (t) over barZ events and a same-sign dilepton analysis of t (t) over barV (V = W or Z) events. In the trilepton channel a direct measurement of the t (t) over barZ cross section sigma(t (t) over barZ) = 0.28(-0.11)(+0.14) (stat)(-0.03)(+0.06) (syst) pb is obtained. In the dilepton channel a measurement of the t (t) over barV cross section yields sigma(t (t) over barV) = 0.43(-0.15)(+0.17) (stat)(-0.07)(+0.09) (syst) pb. These measurements have a significance, respectively, of 3.3 and 3.0 standard deviations from the background hypotheses and are compatible, within uncertainties, with the corresponding next-to-leading order predictions of 0.137(-0.016)(+0.012) and 0.306(-0.053)(+0.031) pb.

Physical Review Letters 110[17], 172002, 2013. DOI: 10.1103/PhysRevLett.110.172002

[P148-13] "Measurement of electrons from beauty hadron decays in pp collisions at root s=7 TeV"

Abelev, B.; Adam, J.; Adamova, D.; Adare, A. M.; Aggarwal, M. M.; **Chinellato, D. D.*; Dash, A.*; Takahashi, J.***; et al.
ALICE Collaboration

The production cross section of electrons from semileptonic decays of beauty hadrons was measured at mid-rapidity (vertical bar y vertical bar < 0.8) in, the transverse momentum range 1 < p(T) < 8 GeV/c with the ALICE experiment at the CERN LHC in pp collisions at a center of mass energy root s = 7 TeV using an integrated luminosity of 2.2 nb(-1). Electrons from beauty hadron decays were selected based on the displacement of the decay vertex from the collision vertex. A perturbative QCD calculation agrees with the measurement within uncertainties. The data were extrapolated to the full phase space to determine the total cross section for the production of beauty quark-antiquark pairs.

Physics Letters B 721[1-3], 13-23, 2013. DOI: 10.1016/j.physletb.2013.01.069

[P149-13] "Measurement of the W+W- and ZZ production cross sections in pp collisions at root s=8 TeV"

Chatrchyan, S.; Khachatryan, V.; Sirunyan, A. M.; Tumasyan, A.; **Chinellato, J.***; et al.
CMS Collaboration

The W+W- and ZZ production cross sections are measured in proton-proton collisions at root s = 8 TeV with the CMS experiment at the LHC in data samples corresponding to an integrated luminosity of up to 5.3 fb(-1). The measurements are performed in the leptonic decay modes W+W- -> l'vl '' v and ZZ -> 2l2l', where l = e, mu and l'(l '') = e, mu, tau. The measured cross sections sigma (pp -> W+W-) =, 69.9 +/- 2.8 (stat.) +/- 5.6 (syst.) 3.1 +/- (lum.) pb and sigma (pp -> ZZ) = 8.4 +/- 1.0 (stat) +/- 0.7 (syst) +/- 0.4 (lum.) pb, for both Z bosons produced in the mass region 60 < m(Z) < 120 GeV, are consistent with standard model predictions. These are the first measurements of the diboson production cross sections at root s = 8 TeV.

Physics Letters B 721[4-5], 190-211, 2013. DOI: 10.1016/j.physletb.2013.03.027

[P150-13] "Measuring red blood cell aggregation forces using double optical tweezers"

Fernandes, H. P.; Fontes, A.; **Thomaz, A.***; Castro, V.; **Cesar, C. L.***; Barjas-Castro, M. L.

Classic immunohematology approaches, based on agglutination techniques, have been used in manual and automated immunohematology laboratory routines. Red blood cell (RBC) agglutination depends on intermolecular attractive forces (hydrophobic bonds, Van der Walls, electrostatic forces and hydrogen bonds) and repulsive interactions (zeta potential). The aim of this study was to measure the force involved in RBC aggregation using double optical tweezers, in normal serum, in the presence of erythrocyte antibodies and associated to agglutination potentiator solutions

(Dextran, low ionic strength solution [LISS] and enzymes). The optical tweezers consisted of a neodymium:yattrium aluminium garnet (Nd:YAG) laser beam focused through a microscope equipped with a minicam, which registered the trapped cell image in a computer where they could be analyzed using a software. For measuring RBC aggregation, a silica bead attached to RBCs was trapped and the force needed to slide one RBC over the other, as a function of the velocities, was determined. The median of the RBC aggregation force measured in normal serum (control) was 1 x 10(-3) (0.1-2.5) poise. cm. The samples analyzed with anti-D showed 2 x 10(-3) (1.0-4.0) poise. cm ($p<0.001$). RBC diluted in potentiator solutions (Dextran 0.15%, Bromelain and LISS) in the absence of erythrocyte antibodies, did not present agglutination. High adherence was observed when RBCs were treated with papain. Results are in agreement with the imunohematological routine, in which non-specific results are not observed when using LISS, Dextran and Bromelain. Nevertheless, false positive results are frequently observed in manual and automated microplate analyzer using papain enzyme. The methodology proposed is simple and could provide specific information with the possibility of meansuration regarding RBC interaction.

Scandinavian Journal Of Clinical & Laboratory Investigation 73[3], 262-264, 2013. DOI: 10.3109/00365513.2013.765961

[P151-13] "Mesoscopic hydro-thermodynamics of phonons in semiconductors: Heat transport in III-nitrides"

Rodrigues, C.G., **Vasconcellos, Á.R.*, Luzzi, R.***

It is presented a generalized hydro-thermodynamics (called mesoscopic hydro-thermodynamics MHT) of phonons in semiconductors, driven away from equilibrium by external forces, derived by the method of moments from a generalized Peierls-Boltzmann kinetic equation built in the framework of a non-equilibrium statistical ensemble formalism. The resulting MHT involves the enormous set of coupled evolution equations for the densities of the quasi-particles (phonons) and their energy together with their fluxes of all orders. The handling of them requires the introduction of a contraction of description what defines MHT's of different orders. We illustrate the matter analyzing heat transport by phonons in GaN within the framework of a MHT of first order to obtain a generalized Guyer-Krumhansl equation from which it is analyzed the effect of geometry on the heat transport. It is described the influence of size (from bulk to nanometric scales) on the reduction of the thermal conductivity and the improving of the figure of merit of thermoelectric devices.

European Physical Journal B 86[5], 200, 2013. DOI: 10.1140/epjb/e2013-40109-1

[P152-13] "Micro-Raman Spectroscopic Characterization of a CR-39 Detector"

Pereira, L. A. S.; Saenz, C. A. T.; Constantino, C. J. L.; Curvo, E. A. C.; Dias, A. N. C.; Soares, C. J.; **Guedes, S.***

Characterization by micro-Raman spectroscopy of polymeric materials used as nuclear track detectors reveals physico-chemical and morphological information on the material's molecular structure. In this work, the nuclear track detector poly(allyl diglycol carbonate), or Columbia Resin 39 (CR-39), was characterized according to the fluence of alpha particles produced by a Ra-226 source and chemical etching time. Therefore, damage of the CR-39 chemical structure due to the alpha-particle interaction with the detector was analyzed at the molecular level. It was observed that the ionization and molecular excitation of the CR-39 after the irradiation process entail cleavage of chemical bonds and formation of latent track. In addition, after the chemical etching, there is also loss of polymer structure, leading to the decrease of the group density C-O-C (similar to 888 cm(-1)), CH=CH (similar to 960 cm(-1)), C-O (similar to 1110 cm(-1)), C-O-C (similar to 1240 cm(-1)), C-O (similar to 1290 cm(-1)), C=O (similar to 1741 cm(-1)), -CH2- (similar to 2910 cm(-1)), and the main band -CH2- (similar to 2950 cm(-1)). The analyses performed after irradiation and chemical etching led to a better understanding of the CR-39 molecular structure and better comprehension of the process of the formation of the track, which is related to chemical etching kinetics.

Applied Spectroscopy 67[4], 404-408, 2013. DOI: 10.1366/12-06741

[P153-13] "Mirror symmetries in multiple diffraction patterns of face-centred cubic crystals"

Parente, C. B. R.; Mazzocchi, V. L.; Sasaki, J. M.; **Cardoso, L. P.***

In this work, a study of the mirror symmetries appearing in multiple diffraction patterns of face-centred cubic crystals is carried out. Several different X-ray and neutron multiple diffraction patterns have been simulated for different face-centred cubic structures. The patterns were plotted in circular plots which showed that two types of symmetry mirrors coexist in the patterns: isomorphic and anamorphic mirrors. The number and types of mirrors depend on the n-fold symmetry of the scattering vector associated with the primary reflection. For n even, only n isomorphic mirrors appear in the patterns. For n odd, n isomorphic mirrors are formed intercalated between n anamorphic mirrors.

Journal Of Applied Crystallography 45, 621-626, Part: 4, 2012. DOI: 10.1107/S0021889812026830

[P154-13] "Net-Charge Fluctuations in Pb-Pb Collisions at root s(NN)=2.76 TeV"

Abelev, B.); Adam, J.; Adamova, D.; Adare, A. M.; Aggarwal, M. M.; **Rinella, G. A.; Chinellato, D. D.*; Dash, A.*; Takahashi, J.***; et al.
ALICE Collaboration

We report the first measurement of the net-charge fluctuations in Pb-Pb collisions at root s(NN) = 2.76 TeV, measured with the ALICE detector at the CERN Large Hadron Collider. The dynamical fluctuations per unit entropy are observed to decrease when going from peripheral to central collisions. An additional reduction in the amount of fluctuations is seen in comparison to the results from lower energies. We examine the dependence of fluctuations on the pseudorapidity interval, which may account for the dilution of fluctuations during the evolution of the system. We find that the fluctuations at the LHC are smaller compared to the measurements at the BNL Relativistic Heavy Ion Collider, and as such, closer to what has been theoretically predicted for the formation of a quark-gluon plasma.

Physical Review Letters 110[15], 152301, 2013. DOI: 10.1103/PhysRevLett.110.152301

[P155-13] "Observation of a muon excess following a gamma-ray burst event detected at the International Space Station"

Augusto, C.R.A., Kopenkin, V., Navia, C.E., De Oliveira, M., Tsui, K.H., **Fauth, A.C.***, Sinzi, T.

On April 24, 2012, at 16:47:14 UT, the Gas Slit Camera (GSC) of the Japanese Monitor of All-sky X-ray Image (MAXI) instrument on the International Space Station detected a short x-ray transient lasting about 34 seconds. The MAXI/GSC transient was most likely a gamma--ray burst (GRB), because of the high Galactic latitude,

spectral hardness ratio, and the absence of known bright x-ray sources at the detected position. In addition, the MAXI/GSC transient GRB 120424A coordinates were in the field of view of the inclined Tupi muon telescope located at ground level (3 m above sea level) at (22.9 W, 43.2 S) in the South Atlantic Anomaly region. We report here that the Tupi telescope registered a muon excess with a signal significance 6.2σ within the MAXI/GSC transient time period. Assuming a power law function with a spectral index of γ=-1.54 in the tail of the primary gamma-ray energy spectrum, we can conclude that the fluence obtained from the muon excess detected by the Tupi telescope is consistent with the preliminary value obtained by the MAXI team. This result agrees with an assumption that the muons were produced in photonuclear reactions in the Earth's atmosphere. In addition, we show also that the South Atlantic Anomaly region can be a favorable place at ground for the detection of the tail of the energy spectrum (the GeV counterpart) of some GRBs.

Physical Review D - Particles, Fields, Gravitation and Cosmology 87[10], 103003, 2013. DOI: 10.1103/PhysRevD.87.103003

[P156-13] "Observation of an Energy-Dependent Difference in Elliptic Flow between Particles and Antiparticles in Relativistic Heavy Ion Collisions"

Adamczyk, L.; Adkins, J. K.; Agakishiev, G.; Aggarwal, M. M.; Ahammed, Z.; **Derradi de Souza, R.*; Takahashi, J.*; Vasconcelos, G. M. S.*;** et al.
Star Collaboration

Elliptic flow (v(2)) values for identified particles at midrapidity in Au + Au collisions, measured by the STAR experiment in the beam energy scan at RHIC at root s(NN) = 7.7-62.4 GeV, are presented. A beamenergy-dependent difference of the values of v(2) between particles and corresponding antiparticles was observed. The difference increases with decreasing beam energy and is larger for baryons compared to mesons. This implies that, at lower energies, particles and antiparticles are not consistent with the universal number-of-constituent-quark scaling of v(2) that was observed at root s(NN) = 200 GeV.

Physical Review Letters 110[14], 142301, 2013. DOI: 10.1103/PhysRevLett.110.142301

[P157-13] "Optical phonon modes of wurtzite InP"

Gadret, E. G.*; de Lima, M. M.; Madureira, J. R.; **Chiaramonte, T.*; Cotta, M. A.*; Iikawa, F.***; Cantarero, A.

Optical vibration modes of InP nanowires in the wurtzite phase were investigated by Raman scattering spectroscopy. The wires were grown along the [0001] axis by the vapor-liquid--solid method. The A(1)(TO), E-2h, and E-1(TO) phonon modes of the wurtzite symmetry were identified by using light linearly polarized along different directions in backscattering configuration. Additionally, forbidden longitudinal optical modes have also been observed. Furthermore, by applying an extended 11-parameter rigid-ion model, the complete dispersion relations of InP in the wurtzite phase have been calculated, showing a good agreement with the Raman experimental data.

Applied Physics Letters 102[12], 122101, 2013. DOI: 10.1063/1.4798324

[P158-13] "Optical spin-to-orbital plasmonic angular momentum conversion in subwavelength apertures"

Brandao, P. A.*; Cavalcanti, S. B.

Within the framework of the Huygens-Fresnel approach, we evaluate the coherent superposition of surface plasmon (SP) modes excited by an incident circularly polarized light propagating through an array of subwavelength holes. Numerical results of the plasmonic distribution exhibit a rich structure that reveals the creation and annihilation of vortex arrays in the field phase. These phase singularities stem from total transfer of the spin angular momentum (AM) of the incident radiation to the orbital AM of the SP.

Optics Letters 38[6], 920-922, 2013. DOI: 10.1364/OL.38.000920

[P159-13] "Photoelectron diffraction study of Rh nanoparticles growth on Fe 3O4/Pd(111) ultrathin film"

Abreu, G.J.P.*, Pancotti, A., **De Lima, L.H.*, Landers, R.*, De Siervo, A.***

Metallic nanoparticles (NPs) supported on oxides thin films are commonly used as model catalysts for studies of heterogeneous catalysis. Several 4d and 5d metal NPs (for example, Pd, Pt and Au) grown on alumina, ceria and titania have shown strong metal support interaction (SMSI), for instance the encapsulation of the NPs by the oxide. The SMSI plays an important role in catalysis and is very dependent on the support oxide used. The present work investigates the growth mechanism and atomic structure of Rh NPs supported on epitaxial magnetite Fe3O4(111) ultrathin films prepared on Pd(111) using the Molecular Beam Epitaxy (MBE) technique. The iron oxide and the Rh NPs were characterized using X-ray photoelectron spectroscopy (XPS), low-energy electron diffraction and photoelectron diffraction (PED). The combined XPS and PED results indicate that Rh NPs are metallic, cover approximately 20 % of the iron oxide surface and show height distribution ranging 3-5 ML (monolayers) with essentially a bulk fcc structure.

Journal of Nanoparticle Research 15[4], 1510, 2013. DOI: 10.1007/s11051-013-1510-z

[P160-13] "Quaternions, hexadecanions and the Schur complement in quantum mechanics"

Mizrahi, S. S.; **de Oliveira, M. C.***

We review the mathematical object invented by Sir William Rowan Hamilton, which he called quaternion, and we study its association with the matrix structure known as complement of Schur. We analyze the positivity of quaternions when represented by 2x2 matrices. We extend this very concept to the larger mathematical object, which generalizes the quaternion, the hexadecanion, which we shall define and use. We apply Schur's method to a quantum state that describes a beam of particles characterized by discrete degrees of freedom, the internal parity and the spin, as proposed by Lee and Yang (1956 Phys. Rev. 104 822).

Physica Scripta T153, 014048, 2013. DOI: 10.1088/0031-8949/2013/T153/014048

[P161-13] "Raman spectroscopy as a probe of molecular order, orientation, and stacking of fluorinated copper-phthalocyanine (F16CuPc) thin films"

Cerdeira, F.*; Garriga, M.; Alonso, M. I.; Osso, J. O.; Schreiber, F.; Dosch, H.; Cardona, M.

We report Raman scattering measurements on azimuthally ordered thin films of F16CuPc, prepared by organic molecular beam deposition on A-plane sapphire substrates. The observed peak frequencies have been compared both to the results of a model calculation for the vibrational modes of the free molecule and to those reported by other authors in related materials. This analysis provides a plausible identification of the modes responsible for the strongest spectral features. Detailed evaluation of the spectra reveals that some observed modes, which correspond to vibrations of the macrocycle inner ring,

largely retain the intramolecular character and their polarisation properties can be used to study the orientation and stacking configuration of the molecules. We provide structural parameters deduced either in molecular or crystal symmetry considering the simpler possibilities, i.e. a single column molecular stacking and a herringbone-like structure. The results suggest that the thicker and most ordered film is structurally close to the recently reported crystal organisation of bulk ribbon samples of this compound. The crystalline quality of the ordered films is mainly reflected in some other Raman peaks which are related to the motion of peripheral atoms and dominate the high wavenumber part of the spectra. These modes are affected by intermolecular interactions inducing Davydov splittings that are unequivocally identified by the observed Raman selection rules. The performed analysis also provides quantitative estimates of the degree of in-plane ordering.

Journal Of Raman Spectroscopy 44[4], 597-607, 2013. DOI: 10.1002/jrs.4231

[P162-13] "RCD Large Aspect-Ratio Tokamak Equilibrium with Magnetic Islands: a Perturbed Approach"

Braga, F. L.*

Solutions of Grad Shafranov (GS) equation with Reversed Current Density (RCD) profiles present magnetic islands when the magnetic flux is explicitly dependent on the poloidal angle. In this work it is shown that a typical cylindrical (large aspect-ratio) RCD equilibrium configuration perturbed by the magnetic field of a circular loop (simulating a divertor) is capable of generate magnetic islands, due to the poloidal symmetry break of the GS equilibrium solution.

Communications In Theoretical Physics 59[3], 375-378, 2013. DOI: 10.1088/0253-6102/59/3/22

[P163-13] "Search for new physics in final states with a lepton and missing transverse energy in pp collisions at the LHC"

Chatrchyan, S.; Khachatryan, V.; Sirunyan, A. M.; Tumasyan, A.; Adam, W.; Aguilo, E.; **Chinellato, J.***; et al.
CMS Collaboration

This Letter describes the search for an enhanced production rate of events with a charged lepton and a neutrino in high-energy pp collisions at the LHC. The analysis uses data collected with the CMS detector, with an integrated luminosity of 5.0 fb(-1) at root s = 7 TeV, and a further 3.7 fb(-1) at root s = 8 TeV. No evidence is found for an excess. The results are interpreted in terms of limits on a heavy charged gauge boson (W') in the sequential standard model, a split universal extra dimension model, and contact interactions in the helicity-nonconserving model. For the last, values of the binding energy below 10.5 (8.8) TeV in the electron (muon) channel are excluded at a 95% confidence level. Interpreting the l(nu) final state in terms of a heavy W' with standard model couplings, masses below 2.90 TeV are excluded.

Physical Review D 87[7], 072005, 2013. DOI: 10.1103/PhysRevD.87.072005

[P164-13] "Simulating Pump-Probe Photoelectron and Absorption Spectroscopy on the Attosecond Timescale with Time-Dependent Density Functional Theory"

De Giovannini, U.; **Brunetto, G.***; Castro, A.; Walkenhorst, J.; Rubio, A.

Molecular absorption and photoelectron spectra can be efficiently predicted with real-time time-dependent density functional theory.

We show herein how these techniques can be easily extended to study time-resolved pumpprobe experiments, in which a system response (absorption or electron emission) to a probe pulse is measured in an excited state. This simulation tool helps with the interpretation of fast-evolving attosecond time-resolved spectroscopic experiments, in which electronic motion must be followed at its natural timescale. We show how the extra degrees of freedom (pump-pulse duration, intensity, frequency, and time delay), which are absent in a conventional steady-state experiment, provide additional information about electronic structure and dynamics that improve characterization of a system. As an extension of this approach, time-dependent 2D spectroscopy can also be simulated, in principle, for large-scale structures and extended systems.

Chemphyschem 14[7], SI, 1363-1376, 2013. DOI: 10.1002/cphc.201201007

[P165-13] "Single Ionization of Liquid Water by Protons, Alpha Particles, and Carbon Nuclei: Comparative Analysis of the Continuum Distorted Wave Methodologies and Empirical Models"

Bernal-Rodriguez, M. A.*; Liendo, J. A.; Belkic D.(Ed.)

Single ionization of liquid water by the impact of fast, but nonrelativistic heavy charged particles is reviewed. Special attention is focused on protons, alpha particles, and carbon ions. This phenomenon has been extensively studied by using theoretical methods during the last decades. Quantum-mechanical as well as semiclassical approaches have been developed. Nevertheless, experimental studies in this field are very scarce. Based upon both theoretical and experimental results, semiempirical formalisms have been reported. At the beginning, the first Born (B1) approximation emerged with some success in reproducing ionization cross sections corresponding to impact energies above a few hundreds of keV/u. The introduction of the distorted-wave formalism brought a remarkable improvement with respect to B1, mainly because of reproduction of the well-known two-center effects. The B1 approximation is treated here in order to be used as a reference model for all the subsequent comparisons. Also presented are the distorted--wave formalism and its variants. On the other hand, available experimental works for measuring ionization cross sections corresponding to water vapor targeted by hydrogen, helium, and carbon ions are summarized. In addition, the most relevant semiempirical approaches intended to calculate water ionization cross sections are addressed. Some of the experimental single ionization cross sections mentioned above are compared to those determined by the distorted-wave and semiempirical formalisms for liquid water. Finally, perspectives on the studies of the ionization problem are briefly commented.

Theory Of Heavy Ion Collision Physics In Hadron Therapy, Serie: Advances in Quantum Chemistry 65, 203-229, 2013. DOI: 10.1016/B978-0-12-396455-7.00008-X

[P166-13] "Solar cells from upgraded metallurgical-grade silicon purified by metallurgical routes"

Cortes, A. D. S.; **Silva, D. S.*; Viana, G. A.*; Motta, E. F.***; Zampieri, P. R.; Mei, P. R.; **Marques, F. C.***

We report a combination of metallurgical routes intended to improve the purity of metallurgical grade silicon (MG-Si) for solar cell fabrication. Initially, MG-Si was submitted to vacuum degassing (VD) by means of an electron-beam to reduce the impurities represented by chemical elements with high vapour pressure. This was followed by preparing a monocrystalline ingot using the Czochralski (CZ) growth technique. The impurity concentration was measured by glow discharge mass spectrometry. The results demonstrate that a procedure combining VD with CZ growth has the potential to improve the purity of MG-Si to greater than 99.999%.

Solar cells made by different processes were used for the sake of comparison and also to verify the quality of the silicon wafers prepared by the combination of VD with CZ techniques. The results showed the potential to reach efficiencies necessary for the production of commercial solar panels.

Journal Of Renewable And Sustainable Energy 5[2], 023129, 2013. DOI: 10.1063/1.4800200

[P167-13] "Stochastic neutrino mixing mechanism"

Guzzo, M. M.*; de Holanda, P. C.*; Peres, O. L. G.*; Zavanin, E. M.*

We propose a mechanism which provides an explanation of the Gallium and antineutrino reactor anomalies. Differently from original Pontecorvo's hypothesis, this mechanism is based on the phenomenological assumption in which the admixture of neutrino mass eigenstates in the moments of neutrino creation and detection can assume different configurations around the admixture parametrized by the usual values of the mixing angles theta(12), theta(23), and theta(13). For simplicity, we assume a Gaussian distribution for the mixing angles in such a way that the average value of this distribution is given by the usual values of the mixing angles, and the width of the Gaussian is denoted by alpha. We show that the proposed mechanism provides a possible explanation for very short-baseline neutrino disappearance, necessary to accommodate Gallium and antineutrino reactor anomalies, which is not allowed in usual neutrino oscillations based on Pontecorvo's original hypotheses. We also can describe high-energy oscillation experiments, like LSND, Fermi, and NuTeV, assuming a weakly energy dependent width parameter, alpha(E), that nicely fits all experimental results.

Physical Review D 87[9], 093003, 2013. DOI: 10.1103/PhysRevD.87.093003

[P168-13] "Study of the underlying event at forward rapidity in pp collisions at sqrt(s) = 0.9, 2.76, and 7 TeV"

S. Chatrchyan, S.; Khachatryan, V.; Sirunyan, A. M.; Tumasyan, A.; Chatrchyan, S.; **Chinellato, J.*** ; et al.
CMS Collaboration

The underlying event activity in proton-proton collisions at forward pseudo-rapidity (−6.6 < η < −5.2) is studied with the CMS detector at the LHC, using a novel observable: the ratio of the forward energy density, dE/dη, for events with a charged-particle jet produced at central pseudorapidity (|η jet| < 2) to the forward energy density for inclusive events. This forward energy density ratio is measured as a function of the central jet transverse momentum, p T, at three different pp centre-of-mass energies (s√=0.9 , 2.76, and 7 TeV). In addition, the s√ evolution of the forward energy density is studied in inclusive events and in events with a central jet. The results are compared to those of Monte Carlo event generators for pp collisions and are discussed in terms of the underlying event. Whereas the dependence of the forward energy density ratio on jet p T at each s√ separately can be well reproduced by some models, all models fail to simultaneously describe the increase of the forward energy density with s√ in both inclusive events and in events with a central jet.

Journal of High Energy Physics 1304[072], 2013. DOI: 10.1007/JHEP04(2013)072

[P169-13] "Synthesis, structural and magnetic characterization of highly ordered single crystalline BiFeO3 nanotubes"

de Oliveira, L. A. S.*; Pirota, K. R.*

In this work, we report on the fabrication of highly ordered single crystalline BiFeO3 (BFO) nanotubes by a sol-gel technique using two-step anodic aluminum oxide (AAO) as template. We prepared BFO nanotubes with dimensions of 65 nm in diameter and 3 mu m in length, as confirmed by scanning electron microscopy (SEM) measurements. The obtained single crystalline nanotubes present the expected pure phase (BiFeO3) as confirmed by energy-dispersive X-ray spectroscopy (EDX), selected area electron diffraction (SAED) and high-resolution transmission electron microscopy (HRTEM). In addition to the antiferromagnetic behavior, the magnetization curves of the BFO nanotubes also present a ferromagnetic response, which holds from 2 to 300 K. This desirable behavior is associated to the break of the antiferromagnetic helical spin ordering of the BFO nanotubes. Besides the magnetocrystalline anisotropy, the large length-to-diameter ratio induced an uniaxial shape anisotropy, attested by the applied magnetic field angle measurements.

Materials Research Bulletin 48[4], 1593-1597, 2013. DOI: 10.1016/j.materresbull.2012.12.066

[P170-13] "Techniques for measuring aerosol attenuation using the Central Laser Facility at the Pierre Auger Observatory"

Abreu, P.; Aglietta, M.; Ahlers, M.; Ahn, E. J.; Albuquerque, I. F. M.; **Batista, R. Alves*; Chinellato, J. A.*; Daniel, B.*; de Mello, W. J. M., Jr.*; Dobrigkeit, C.*; Escobar, C. O.*; Fauth, A. C.*; Kemp, E.*; Muller, M. A.*; Selmi-Dei, D. Pakk*; Silva, M. Zimbres*;** et al.
Pierre Auger Collaborat

The Pierre Auger Observatory in Malargue, Argentina, is designed to study the properties of ultra-high energy cosmic rays with energies above 10(18) eV. It is a hybrid facility that employs a Fluorescence Detector to perform nearly calorimetric measurements of Extensive Air Shower energies. To obtain reliable calorimetric information from the FD, the atmospheric conditions at the observatory need to be continuously monitored during data acquisition. In particular, light attenuation due to aerosols is an important atmospheric correction. The aerosol concentration is highly variable, so that the aerosol attenuation needs to be evaluated hourly. We use light from the Central Laser Facility, located near the center of the observatory site, having an optical signature comparable to that of the highest energy showers detected by the FD. This paper presents two procedures developed to retrieve the aerosol attenuation of fluorescence light from CLF laser shots. Cross checks between the two methods demonstrate that results from both analyses are compatible, and that the uncertainties are well understood. The measurements of the aerosol attenuation provided by the two procedures are currently used at the Pierre Auger Observatory to reconstruct air shower data.

Journal of Instrumentation 8, P04009, 2013. DOI: 10.1088/1748-0221/8/04/P04009

[P171-13] "The competing effect of ammonia in the synthesis of iron oxide/silica nanoparticles in microemulsion/sol-gel system"

Fernandes, M. T. C.; Garcia, R. B. R.; **Leite, C. A. P.***; Kawachi, E. Y.

Combined microemulsion/sol-gel processes may be used to prepare composite nanoparticles. In this work, iron oxide/silica nanoparticles were synthesized in such a combined system, having ammonium hydroxide acting in both processes: as precipitating agent in the synthesis of iron oxide and as catalyst in the sol-gel process of silica. The nanoparticles were synthesized in microemulsions containing tetraethoxysilane (TEOS) and composed by Triton X-100/hexyl alcohol/cyclohexane/aqueous solution, with different amounts of ammonium hydroxide.

Powder materials were obtained after centrifugation, washing and drying, and they were analyzed as synthesized and after heating at 350, 500 and 1000 degrees C. The influence of base quantity was evaluated in relation to the size of the particles and the iron oxide phase synthesized. TEM analysis showed that nanometric iron oxide particles were formed and that they were percolated by a net of amorphous silica. The higher amount of ammonia seems to have induced TEOS condensation process instead of iron oxide particles' growth, indicating that the quantity of base influenced both the microemulsion system and the sal-gel process, but with minor influence over the iron oxide composition, as evidenced by FT-IR and DRX.

Colloids and Surfaces A-Physicochemical And Engineering Aspects 422, 136-142, 2013. DOI: 10.1016/j.colsurfa.2013.01.025

[P172-13] "The role of sex separation in neutral speciation"

Baptestini, E. M.*; de Aguiar, M. A. M.*; Bar-Yam, Y.

Neutral speciation mechanisms based on isolation by distance and assortative mating, termed topopatric, has recently been shown to describe the observed patterns of abundance distributions and species-area relationships. Previous works have considered this type of process only in the context of hermaphroditic populations. In this work, we extend a hermaphroditic model of topopatric speciation to populations where individuals are explicitly separated into males and females. We show that for a particular carrying capacity, speciation occurs under similar conditions, but the number of species generated is lower than in the hermaphroditic case. As a consequence, the species-area curve has lower exponents, especially at intermediate scales. Evolution results in fewer species having more abundant populations.

Theoretical Ecology 6[2], 213-223, 2013. DOI: 10.1007/s12080-012-0172-2

[P173-13] "Theory of High Temperature Superconductivity Beyond BCS with Realistic Coulomb and Frohlich Interactions"

Alexandrov, A. S.*

Along with some other researches we have realised that the true origin of high-temperature superconductivity is found in the strong Coulomb repulsion combined with a significant electron-phonon interaction. Both interactions are strong (on the order of 1 eV) compared with the low Fermi energy of doped carriers which makes the conventional BCS-Eliashberg theory inapplicable in cuprates and related doped insulators. Based on our recent analytical and numerical results we argue that high-temperature superconductivity from repulsion alone is impossible for any strength of the Coulomb interaction. Major steps of the alternative polaron theory are outlined starting from the generic Hamiltonian including the unscreened (bare) Coulomb and electron-phonon interactions. The theory accounts for high superconducting critical temperatures, unconventional isotope effects and reconciles tunnelling, photoemission and quantum oscillation data.

Journal Of Superconductivity And Novel Magnetism 26[4], SI, 1313-1317, 2013. DOI: 10.1007/s10948-012-2098-8

[P174-13] "Thickness alterations of CR-39 plastic detectors due to the heating influence: Basic theory and experimental results"

Rana, M.A., **Guedes, S.***, Iqbal, M.

Heating experiments were conducted on CR-39 polymer/plastic detector samples at temperatures between 50 and 175 °C for various time intervals from 5 to 210 min to investigate the thermal behavior of detector material. Mass and thickness of un-heated and heated polymer samples were measured. Three distinct regimes have been observed showing different degrees of changes in thickness and mass of annealed samples. The percent change of thickness was considerably higher than the mass change during heating. Thermodynamic concepts are used to explain the experimentally observed heating regimes. Role of the difference between free energies of lateral and fold surfaces in detector thickening during heating is discussed. Scanning electron microscopy (SEM) was carried out on un-heated and heated CR-39 samples to examine the surface alterations due to heating. Results are useful for researchers who employ track detectors for radiation measurements in nuclear reactors and cosmic rays. They are also interesting for researchers in related fields, like fission track dating, which consider the thermal history of track recording materials. Our quantitative data and SEM imaging suggests that structural changes, especially surface changes in CR-39 polymer are very important and need to be explored carefully through joint SEM and the Atomic Force Microscopy (AFM).

Radiation Measurements 50, 87-91, 2013. DOI: 10.1016/j.radmeas.2012.07.014

[P175-13] "Traveling wave current drive theory for an arbitrary m-polar configuration"

Duarte, V. N.; **Clemente, R. A.*;** Farengo, R.

An extension of the formalism employed to describe current drive in magnetized plasmas by means of traveling magnetic fields (or double-helix configuration) is presented. In all previous theoretical studies, only driving fields with dipolar topology have been employed and the figure of merit of the current drive mechanism has never been analyzed in terms of the dissipation in the power feeding circuit. In this paper, we show how to express the model equations in terms of the current amplitude in the coils, for an arbitrary number of equally spaced coils wound around the plasma column. We present a brief review of the existing theory and a theoretical formulation, valid for an arbitrary m-polar helical symmetry, which removes the above mentioned complications and limitations. In the limit of straight coils, our magnetic field expression agrees exactly with well-established results of the literature for rotating magnetic field current drive. Finally, we present initial numerical results from a recently developed code which consistently compares the steady driven nonlinear Hall currents and steady fields, corresponding to different configurations in terms of the Ohmic dissipation in the helical coils and discuss future perspectives.

Physics Of Plasmas 20[3], 032513, 2013. DOI: 10.1063/1.4796089

[P176-13] "U(1) x SU(2) gauge invariance leading to charge and spin conductivity of Dirac fermions in grapheme"

Dartora, C. A.; **Cabrera, G. G.***

Gauge symmetries have been identified in graphene and associated with specific physical properties. For instance, the U(1) gauge group is related to electrodynamics in (1 + 2)-dimensional [(1 + 2) D] space-time and non-Abelian gauge groups can describe curvature and torsion. Here we demonstrate that the Dirac Lagrangian for massless electrons near the Dirac points is also invariant under the group SU(2) related to local spin rotations, leading to the correct spin-orbit interactions and a rigorous definition for the spin-current density. Furthermore, we computed the charge and spin conductivity within the framework of Kubo linear response theory, using the algebra of relativistic Dirac spinors in (1 + 2) D space-time.

The minimal value of electrical conductivity is predicted to be pi q(2)/h, in agreement with typical experimental findings.

Physical Review B 87[16], 165416, 2013. DOI: 10.1103/PhysRevB.87.165416

[P177-13] "Ultrahigh Energy Neutrinos at the Pierre Auger Observatory"

Abreu, P.); Aglietta, M.; Ahlers, M.; Ahn, E. J.; Albuquerque, I. F. M.; **Alves Batista, R.*; Chinellato, J. A.*; Daniel, B.*; de Mello Junior, W. J. M.*; Dobrigkeit, C.*; Escobar, C. O.*; Fauth, A. C.*; Kemp, E.*; Muller, M. A.*; Pakk Selmi-Dei, D.*; Zimbres Silva, M.***, et al.
Pierre Auger Collaboration

The observation of ultrahigh energy neutrinos (UHE nu s) has become a priority in experimental astroparticle physics. UHE nu s can be detected with a variety of techniques. In particular, neutrinos can interact in the atmosphere (downward-going nu) or in the Earth crust (Earth-skimming nu), producing air showers that can be observed with arrays of detectors at the ground. With the surface detector array of the Pierre Auger Observatory we can detect these types of cascades. The distinguishing signature for neutrino events is the presence of very inclined showers produced close to the ground (i.e., after having traversed a large amount of atmosphere). In this work we review the procedure and criteria established to search for UHE nu s in the data collected with the ground array of the Pierre Auger Observatory. This includes Earth-skimming as well as downward-going neutrinos. No neutrino candidates have been found, which allows us to place competitive limits to the diffuse flux of UHE nu s in the EeV range and above.

Advances In High Energy Physics, 708680, 2013. DOI: 10.1155/2013/708680

[P178-13] "Wess-Zumino supersymmetric phase and superconductivity in grapheme"

Dartora, C. A.; **Cabrera, G. G.***

Supersymmetry is expected to exist in nature at high energies, but must be spontaneously broken at ordinary energy scales. The required energy scale in elementary particle physics is currently inaccessible, but condensed matter could furnish low energy realizations of supersymmetry. In graphene, electrons behave as 'relativistic' massless fermions in 1 + 2 dimensions. Here we propose phenomenologically, assuming that some microscopic parameters can be fine-tuned in graphene, the existence of a supersymmetric Wess-Zumino phase. The supersymmetry breaking leads to a superconductor phase, described by a relativistic Ginzburg-Landau phenomenology.

Physics Letters A 377[12], 907-909, 2013. DOI: 10.1016/j.physleta.2013.02.008

[P179-13] "Zircon fission track and U-Pb dating methods applied to São Paulo and Taubaté Basins located in the southeast Brazil"

Curvo, E.A.C., Tello S., C.A., Carter, A., Dias, A.N.C., Soares, C.J., Nakasuga, W.M., Resende, R.S., Gomes, M.R., **Alencar, I.*, Hadler, J.C.***

Zircon samples from the Cenozoic São Paulo and Taubaté Basins and Mantiqueira Mountain Range (southeast Brazil) were concomitantly dated by zircon Fission Track Method (FTM) and in situ U-Pb dating method. While FTM detrital-zircon data are ideally used to provide low-temperature information, U-Pb single detrital grain ages record the time of zircon formation in igneous or high grade metamorphic environments. This methodology may be used to study the possible sources of the basins sediments. The results suggest that the São Paulo Basin is composed of sediments from just one source, the Mantiqueira Mountain Range. On the other hand, the Taubaté Basin presents further sediment sources besides the Mantiqueira Mountain Range.

Radiation Measurements 50, 172-180, 2013. DOI: 10.1016/j.radmeas.2012.07.015

Proceedings

[P180-13] "Hadronic Cross Sections, Elastic Slope and Physical Bounds"

Fagundes, D. A.*; Menon, M. J.*; Goncalves V. P.(Ed.); Da Silva M. L. L.(Ed.); Amaral J. T. D.(Ed.); Machado M. V. T.(Ed.)

An almost model-independent parametrization for the ratio of the total hadronic cross section to elastic slope is discussed. Its applicability in studies of asymptotia and analyses of extensive air shower in cosmic-ray physics is also outlined.

HADRON PHYSICS CONFERENCE, 12., 2012, Bento Gonçalves, Brasil: Aip Conference Proceedings 1520, 297-299, 2013. DOI: 10.1063/1.4795978

[P181-13] "Hunting for asymptotia at LHC"

Pancheri, G., **Fagundes, D.A.***, Grau, A., Pacetti, S., Srivastava, Y.N.

We discuss whether the behaviour of some hadronic quantities, such as the total crosssection, the ratio of the elastic to the total cross-section, are presently exhibiting the asymptotic behaviour expected at very large energies. We find phenomenological evidence that at LHC7 there is still space for further evolution.

AIP Conference Proceedings 1523, 123-127, 2013. DOI: 10.1063/1.4802132

[P182-13] "Improvement on a new concept of beamline delivering high purity VUV photons starting at 7.3 eV"

Fonseca, P.T., Faleiros, M.M., Moraes, H.R., Souza, L., Rodrigues, G.L.P.M., Chaves, D.S., Ambrósio, C., **De Brito, A.N.***

We report recent improvements and performance on the Toroidal Grating Monochromator (TGM) beamline at the Laboratório Nacional de Luz Síncrotron-LNLS. Compared to normal incidence monochromators, (NIMs), TGMs provide substantially wider energy range, less resolving power and very poor higher harmonic rejection (HHR). A new concept, MIRHACLLE [1], developed at LNLS, allows reaching more than five orders of harmonic rejection (NIM gives 10%). Previously, we were not able to reach below 12 eV using MIRHACLLE. Here we report improvements extending the lower limit to 7.3 eV. Furthermore, HHR is maintained down to the lower limit using a special gas mixture, the upper limit given by 330 eV is kept.

Journal of Physics: Conference Series 425 [PART 12], 122003, 2013. DOI: 10.1088/1742-6596/425/12/122003

[P183-13] "On the unzipping mechanisms of carbon nanotubes: Insights from reactive molecular dynamics simulations"

Dos Santos, R.P., **Autreto, P.A.*, Perim, E.*, Brunetto, G.*, Galvao, D.S.***

Unzipping carbon nanotubes (CNTs) is considered one of the most promising approaches for the controlled and large-scale production of graphene nanoribbons (GNR). These structures are considered of great importance for the development of nanoelectronics because of its dimensions and intrinsic non-zero band gap value. Despite many years of investigations some details on the dynamics of the CNT fracture/unzipping processes remain unclear. In this work we have investigated some of these process through molecular dynamics simulations using reactive force fields (ReaxFF), as implemented in the Large-scale Atomic/Molecular Massively Parallel Simulator (LAMMPS) code. We considered multi-walled CNTs of different dimensions and chiralities and under induced mechanical stretching. Our preliminary results show that the unzipping mechanisms are highly dependent on CNT chirality. Well-defined and distinct fracture patterns were observed for the different chiralities. Armchair CNTs favor the creation of GNRs with well-defined armchair edges, while zigzag and chiral ones produce GNRs with less defined and defective edges.

Materials Research Society Symposium Proceedings 1451, 3-8, 2013. DOI: 10.1557/opl.2012.1329

[P184-13] "Preliminary Results on the Empirical Applicability of the Tsallis Distribution in Elastic Hadron Scattering"

Fagundes, D. A.*; Menon, M. J.*; Goncalves V. P.(Ed.); Da Silva M. L. L.(Ed.); Amaral J. T. D.(Ed.); Machado M. V. T.(Ed.)

We show that the proton-proton elastic differential cross section data at dip position and beyond can be quite well described by a parametrization based on the Tsallis distribution, with only five free fit parameters. Extrapolation of the results obtained at 7 TeV to large momentum transfer, suggests that hadrons may not behave as a black-disk at the asymptotic energy region.

Hadron Physics Conference, 12., 2012, Bento Gonçalves, Brasil: Aip Conference Proceedings 1520, 300-302, 2013. DOI: 10.1063/1.4795979

[P185-13] "Sm3+ effects in the Tm3+ doped tellurite glass for S-band amplification"

Belançon, M.P., Ferenz, J., Chillcce, E., **Barbosa, L.C.***

Thulium doped Samarium codoped tellurite-tungstate glasses were produced. Luminescence properties in the infrared region were investigated looking to observe improved properties for S-band amplification in the co doped samples. Thulium is well-known by the 3H4-3F4 radiative transition emitting around ~1.47μm, which is a self-terminating transition in tellurite hosts due the longer lifetime of the lower level in relation to the upper level of this transition. Analysis of absorption and emission spectra showed that we could quench the 3F4 level significantly, what improved the intensity of the emission at 1.49μm. However, the state 3H4 were also quenched due the cross relaxation process due the absorption bands of Sm3+ around 1.5μm.

Proceedings of SPIE - The International Society for Optical Engineering, 8601, 86012D, 2013. DOI: 10.1117/12.2002897

[P186-13] "Spectroscopic investigation of the glass system TeO2-WO3-Na2O-Nb2O5 for mid-infrared amplifiers"

Belançon, M.P., **Barbosa, L.C.***

Tellurite glasses following the molar concentration 71.5% TeO2, 22.5% WO3, 5% Na2O and 1.5% Nb2O5 have been investigated. Samples doped with Tm2O3, Pr2O3, Yb2O3 or Bi2O3 were fabricated by the conventional melt quenching process. Rare-earth (RE) 3+ ions have well defined emission bands. On the other hand, Bismuth emission in the infrared region have been found in some glasses and even that emission laser have been already obtained, the mechanism behind its luminescence is still misunderstood[1]. The Bismuth emission is sometimes referred as a "superbroadband" emission around 1.3um, which is very promising for an optical amplifier, but, to the best of our knowledge a bismuth based optical amplifier have not been produced yet. Our purpose is to investigate the mechanism behind this misunderstood "superbroadband" luminescence, and compare it with the rare-earths properties in the same range. The characterization consists in measurements of optical absorption spectra, optical emission spectra and life-time decay. Differential thermal analysis (DTA) was also performed, to identify changes in Tg and Tx as function of the doping concentration, which is important to the drawing process of a fiber.

Proceedings of SPIE - The International Society for Optical Engineering, 8601, 86012F, 2013. DOI: 10.1117/12.2003021

[P187-13] "The U11 PGM beam line at the Brazilian National Synchrotron Light Laboratory"

Cezar, J.C., Fonseca, P.T., Rodrigues, G.L.M.P., **De Castro, A.R.B.***, Neuenschwander, R.T., Rodrigues, F., Meyer, B.C., Ribeiro, L.F.S., Moreira, A.F.A.G., Piton, J.R., Raulik, M.A., Donadio, M.P., Seraphim, R.M., Barbosa, M.A., **De Siervo, A.*, Landers, R.*, De Brito, A.N.***

We present the U11 beam line at the National Synchrotron Light Laboratory (LNLS), Brazil. This is the first undulator based beam line installed at the UVX storage ring. It is based on the collimated plane grating monochromator design, which allows for variation in included angle of the grating. The results obtained during the commissioning demonstrate a good overall performance in terms of energy resolution and beam size, in accord with the expected values obtained from ray tracing calculation.

Journal of Physics: Conference Series 425[PART 7], 072015, 2013. DOI: 10.1088/1742-6596/425/7/072015

[P188-13] "When small is different: The case of membranes inside tubes"

Perim, E.*, Fonseca, A.F., **Galvão, D.S.***

Recently, classical elasticity theory for thin sheets was used to demonstrate the existence of a universal structural behavior describing the confinement of sheets inside cylindrical tubes. However, this kind of formalism was derived to describe macroscopic systems. A natural question is whether this behavior still holds at nanoscale. In this work, we have investigated through molecular dynamics simulations the structural behavior of graphene and boron nitride single layers confined into nanotubes. Our results show that the class of universality observed at macroscale is no longer observed at nanoscale. The origin of this discrepancy is addressed in terms of the relative importance of forces and energies at macro and nano scales.

Materials Research Society Symposium Proceedings 1451, 15-20, 2013. DOI: 10.1557/opl.2012.1252

Book Review

"Carl Friedich Gauss and Russia: His Correspondence with Scientists working in Russia"

Assis, A. K. T.*

Science & Education 22[3], 717-721, 2013. DOI: 10.1007/s11191-012-9507-z

Meeting Abstract

"How Well Are Women Represented in Hard Sciences and Technology Majors at the State University of Campinas?"

Vasconcellos, E. D. C.*; Brisolla, S. N.
Cunningham B. A.(Ed.)

Women In Physics, Serie: AIP Conference Proceedings 1517, 175-175, 2013.

Correção

"Analysis Of Crosstalk Between 10 Gb/S X 64 Channels In Two-Pump Fiber Optical Parametric Amplifier (Vol 55, Pg 926, 2013)"

Callegari, F. A.*; Marconi, J. D.*; Fragnito, H. L.*

Originally published Microwave Opt Technol Lett 55:730734, 2013. (c) 2012 Wiley Periodicals, Inc. Microwave Opt Technol Lett 55:1703, 2013; View this article online at wileyonlinelibrary.com. DOI 10.1002/mop.27669 (Original article DOI 10.1002/mop.27449)

Microwave And Optical Technology Letters 55[7], 1703-1703, 2013. DOI: 10.1002/mop.27669

Patente

[Pa002-2013] "Gaspra - Gerador de experimentos para imagens astronômicas"

Gradvohl, A. L. S.; **Andrijauskas, F.***

Número da Patente ou Registro: (Agência INOVA) BR 51 2013 000117 0
Tipo de Programa de computador: computacional
Mês/Ano de Conclusão:02/2013
INPI/BBRASIL

Fonte: SIPEX – Sistema de Informação e Pesquisa e Extensão da nicamp.
Disponível em: http:///wwww.uunicamp.br/ssipex/

Artigos Aceitos para Publicação

[A001-13] "A comparison between neutron-fluence measurements using metal-activation monitors and standard glasses calibrated via thin uranium-fission monitors and via ηq method"

Curvo, E.A.C., Jonckheere, R., **Guedes, S.*, Iunes, P.J.***, Tello, C.A., **Hadler, J.C.***, Unterricker, S., Ratschbacher, L.

The two fundamental approaches to fission-track dating involve either an explicit determination of the thermal neutron fluence (φ-method) or a calibration against age standards (ζ-method). The neutron fluence measurements are carried out with metal-activation monitors or with uranium-fission monitors, co-irradiated with the samples. Uranium-fission monitors consist of either a thin "mono-atomic") film, or a thick fission source (standard uranium glass) irradiated against a muscovite external track detector. In this work, different techniques for performing neutron-fluence measurements were compared: based on thin-film calibration, based on thick-source calibration, and based on gamma spectrometry of co-irradiated metal monitors (Au, Co). The results suggest that more experiments are needed to make all calibrations consistent, including new measurements of the length of etched induced tracks in mica. Also the standard glass calibration carried out with thin films should be confirmed with a greater number of calibrating irradiations.

Radiation Measurements, 2013. DOI: 10.1016/j.radmeas.2013.03.002

[A002-13] "Dose point kernels in liquid water: An intra-comparison between GEANT4-DNA and a variety of Monte Carlo codes"

Champion, C., Incerti, S., Perrot, Y., Delorme, R., Bordage, M.C., Bardiès, M., Mascialino, B., Tran, H.N., Ivanchenko, V., **Bernal, M.***, Francis, Z., Groetz, J.-E., Fromm, M., Campos, L.

Modeling the radio-induced effects in biological medium still requires accurate physics models to describe the interactions induced by all the charged particles present in the irradiated medium in detail. These interactions include inelastic as well as elastic processes. To check the accuracy of the very low energy models recently implemented into the GEANT4 toolkit for modeling the electron slowing-down in liquid water, the simulation of electron dose point kernels remains the preferential test. In this context, we here report normalized radial dose profiles, for mono-energetic point sources, computed in liquid water by using the very low energy "GEANT4-DNA" physics processes available in the GEANT4 toolkit. In the present study, we report an extensive intra-comparison of profiles obtained by a large selection of existing and well-documented Monte-Carlo codes, namely, EGSnrc, PENELOPE, CPA100, FLUKA and MCNPX.

Applied Radiation and Isotopes, 2013. DOI: 10.1016/j.apradiso.2013.01.037

[A003-13] "Energy deposition in small-scale targets of liquid water using the very low energy electromagnetic physics processes of the Geant4 toolkit"

Incerti, S., Champion, C., Tran, H.N., **Karamitros, M*., Bernal, M.***, Francis, Z., Ivanchenko, V., Mantero, A.

In the perspective of building an open source simulation platform dedicated to the modelling of early biological molecular damages due to ionising radiation at the DNA scale, the general-purpose Geant4 Monte Carlo simulation toolkit has been recently extended with specific very low energy electromagnetic physics processes for liquid water medium. These processes - also called "Geant4-DNA" processes - simulate the physical interactions induced by electrons, hydrogen and helium atoms of different charge states. The present work reports on the energy deposit distributions obtained for incident electrons, protons and alpha particles in nanometre-size volumes comparable to those present in the genetic material of mammalian cells. The frequency distributions of the energy deposition obtained for three typical geometries of nanometre-size cylindrical targets placed in a spherical phantom are found to be in reasonable agreement with prior works. Furthermore, we present a combination of the Geant4-DNA processes with a simplified geometrical model of a cellular nucleus allowing the evaluation of energy deposits in volumes of biological interest.

Nuclear Instruments and Methods in Physics Research, Section B: Beam Interactions with Materials and Atoms, 2013. DOI: 10.1016/j.nimb.2012.12.054

[A004-13] "Licensing a fuel cell bus and a hydrogen fueling station in Brazil"

Neves Jr., N.P.*, Pinto, C.S.

The Brazilian Fuel Cell Bus Project is being developed by a consortium comprising 14 national and international partners.

The project was initially supported by the GEF/UNDP and MME/FINEP Brazil. The national coordination is under responsibility of MME and EMTU/SP, the São Paulo Metropolitan Urban Transport Company that also controls the bus operation and bus routes. This work reports the efforts done in order to obtain the necessary licenses to operate the first fuel cell buses for regular service in Brazil, as well as the first commercial hydrogen fueling station to attend the vehicles.

International Journal of Hydrogen Energy, 2013. DOI: 10.1016/j.ijhydene.2013.01.035

[A005-13] "Magnetic properties study of iron-oxide nanoparticles/PVA ferrogels with potential biomedical applications"

Mendoza Zélis, P., **Muraca, D.*,** Gonzalez, J.S., Pasquevich, G.A., Alvarez, V.A., **Pirota, K.R.*,** Sánchez, F.H.

A study of the magnetic behavior of maghemite nanoparticles (NPs) in polyvinyl alcohol (PVA) polymer matrices prepared by physical cross-linking is reported. The magnetic nanocomposites (ferrogels) were obtained by the in situ co-precipitation of iron salts in the presence of PVA polymer, and subsequently subjected to freezing-thawing cycles. The magnetic behavior of these ferrogels was compared with that of similar systems synthesized using the glutaraldehyde. This type of chemical cross-linking agents presents several disadvantages due to the presence of residual toxic molecules in the gel, which are undesirable for biological applications. Characteristic particle size determined by several techniques are in the range 7.9-9.3 nm. The iron oxidation state in the NPs was studied by X-ray absorption spectroscopy. Mössbauer measurements showed that the NP magnetic moments present collective magnetic excitations and superparamagnetic relaxations. The blocking and irreversibility temperatures of the NPs in the ferrogels, and the magnetic anisotropy constant, were obtained from magnetic measurements. An empirical model including two magnetic contributions (large NPs slightly departed from thermodynamic equilibrium below 200 K, and small NPs at thermodynamic equilibrium) was used to fit the experimental magnetization curves. A deviation from the superparamagnetic regime was observed. This deviation was explained on the basis of an interacting superparamagnetic model. From this model, relevant magnetic and structural properties were obtained, such as the magnitude order of the dipolar interaction energy, the NPs magnetic moment, and the number of NPs per ferrogel mass unit. This study contributes to the understanding of the basic physics of a new class of materials that could emerge from the PVA-based magnetic ferrogels.

Journal of Nanoparticle Research 15[5], 1-12, 2013. DOI: 10.1007/s11051-013-1613-6

*** Autores do Instituto de Física "Gleb Wataghin" - IFGW**

Defesa de Dissetações - Mestrado

[D010-13] "Design e caracterização de junções ScS em Nióbio"
Aluno: Felipe Gustavo da Silva Santos
Orientador: Amir Ordacgi Caldeira
Data: 10/05/2013

[D011-13]"Nano agregados metálicos: produção e propriedades magnéticas"
Aluno: Artur Domingues Tavares de Sá
Orientador: Varlei Rodrigues
Data: 21/06/2013

Defesa de Teses - Doutorado

[T005-13] "Simulações atomísticas de nono-estruturas de carbono contendo milhões de átomos"
Leonardo Dantas Machado
Orientador: Douglas Soares Galvão
Data: 14/06/2013

[T006-13] "Busca por assinaturas do campo magnéticos galáctico usando wavelets esféricos"
Aluno: Marcelo Zimbres Silva
Orietnador: Ernesto Kemp
Data: 20/06/2013

Fonte: Portal IFGW/PPós-graduação.
Disponível em: http://portal.ifi.unicamp.br/eventos#date=2013-05-01,mode=month

*** Acesse o portal Abstracta** <http://abstracta.ifi.unicamp.br> e faça seu **cadastro como Leitor** para receber por email as novidades de cada novo número publicado.

Abstracta

Instituto de Física
Diretor: Prof. Dr. Daniel Pereira
Diretor Associado: Prof. Dr. Newton Cesario Frateschi
Universidade Estadual de Campinas - UNICAMP
Cidade Universitária Zeferino Vaz
13083-859 - Campinas - SP - Brasil
e-mail: secdir@ifi.unicamp.br
Fone: 0XX 19 3521-5300

Publicação

Biblioteca do Instituto de Física Gleb Wataghin
http://portal.ifi.unicamp.br/biblioteca

Diretora Técnica: Sandra Maria Carlos Cartaxo
Coordenador da Comissão de Biblioteca: Prof. Dr. André Koch Torres de Assis

Elaboração
Maria Graciele Trevisan (Bibliotecária)
graciele@ifi.unicamp.br

Projeto Gráfico
ÍgneaDesign

Impressão: Gráfica Central - Unicamp